

# Bed forms in bimodal sand–gravel sediments: laboratory and field analysis

R. A. KUHNLE\*, J. K. HORTON†, S. J. BENNETT‡ and J. L. BEST†

\*National Sedimentation Laboratory, PO Box 1157, 598 McElroy Drive, USDA-ARS NSL, Oxford, MS 38655, USA (E-mail: rkuhnle@msa-oxford.ars.usda.gov)

†Earth & Biosphere Institute, School of Earth & Environment, University of Leeds, Leeds, West Yorkshire LS2 9JT, UK

‡Department of Geography, State University of New York at Buffalo, Buffalo, NY 14261, USA

## ABSTRACT

Bed forms were studied in Goodwin Creek and a laboratory flume channel. The bed sediment of the field site and flume had median diameters of 8.3 (modes of 0.4, 22.6 mm) and 1.82 mm (modes of 0.5, 5.6 mm), respectively. The laboratory and field channels had similar values of bimodal parameters, ratios of flow depth to median bed material diameter, and ratios of shear stress to critical shear stress and were judged to be comparable in the transport of bed load sediment and the resulting bed forms. Three groupings of bed forms from the laboratory flume experiments (ripple-like bed forms, bed load sheets, low-relief bed waves) were identified using the height and period of the bed forms. For the range of flow depths and discharges investigated in the flume, bed forms became higher and longer with increasing bed shear stress. Bed forms from Goodwin Creek were similar to those from the flume with comparable ratios between bed form length, height, and flow depth. The bed forms in the flume provide a positive link between rate and size fluctuations measured in the field and the bed forms. The smaller bed forms identified were sediment starved and are not considered to be dunes, while the largest bed forms in which all of the bed material sizes were mobilized in the field and laboratory were judged to be dunes.

**Keywords** Bed forms, bimodal size distribution, sand–gravel sediment, sediment transport.

## INTRODUCTION

Bed forms in gravel-bed streams form as an interaction between the flow and motion of the bed material sediment. These interactions between fluid flow and different size fractions in sediment mixtures control sediment transport, grain-size sorting, flow resistance, and the depositional characteristics of these sediments. These effects are manifested through the development, organization, and migration of various low-relief bed forms. Laboratory studies have documented the nature of initiation of motion and fractional transport of mixtures of sand and gravel in laboratory flumes (Bridge & Bennett, 1992; Kuhnle, 1993; Wilcock & McArdell, 1993; Wilcock, 1997). It has been shown convincingly

that characteristics of the size distribution of the bed material (i.e. bimodal or unimodal) have a strong effect on the initiation of motion and transport of sand–gravel mixtures (Wilcock, 1993; Wilcock & Kenworthy, 2002). Parameters have been derived to characterize whether the range of sizes of the bed material sediment will be entrained over a narrow range of flow strengths (unimodal) or be entrained as a function of size, particularly in the gravel size ranges (bimodal) (Wilcock, 1993; Sambrook Smith *et al.*, 1997). Detailed information on bed forms that form in sub-critical flows in streams with a bed material composed of sand and gravel is usually difficult to collect because of poor water clarity, unpredictable and unsteady flows, and the difficulty of collecting flow and sediment data.

### Previously identified bed forms in sand–gravel sediment

A comprehensive summary of the state of knowledge of dunes in gravel has been published by Carling (1999). Much of the data on dunes in gravel comes from studies by Dinehart (1989, 1992a,b) and Dinehart (1999). Carling concluded that dunes in gravel do exist and concur with classic dune form criteria. It is not entirely clear how bed load sheets (BLS) (Whiting *et al.*, 1988; Kuhnle & Southard, 1990; Bennett & Bridge, 1995b) found in sand and gravel mixtures relate to the dunes in gravel found in other studies (Carling, 1999). BLS generally plot on lower plane or dune bed form existence fields of Southard & Boguchwal (1990) and Allen (1983); however, they have also been measured under supercritical flows (Kuhnle & Southard, 1990) and tend to have lower height to length ratios than other gravel dunes (Carling, 1999).

A summary of the range of flow transverse bed forms that have been previously identified in mixed sized sediment mixtures is contained in Table 1. A heterogeneous sediment mixture is essential for the development of two of the bed form populations observed here, i.e. ripple-like bed forms (RLBF) and BLS. This is exemplified by the flume experiments of Dietrich *et al.* (1989)

where BLS were only apparent with the addition of sand to fine gravel. Furthermore the ratio of the different grain-size fractions is important in the formation of these bed forms (Iseya & Ikeda, 1987; Ikeda & Iseya, 1988). RLBF formed in sand and have heights and lengths that are usually associated with ripples, but occur under rough turbulent flow. BLS were first defined in the literature by Whiting *et al.* (1988), as long and low (metres in length, one to two coarse grains high) waves of moving bed material sediment with coarse fronts and no slip face. Similar long and low bed forms but lacking coarse fronts were described in a laboratory flume study by Kuhnle & Southard (1988). BLS essentially consist of the finer fractions of the bed which move downstream as they fill in the interstices of the coarse-grained 'troughs'. Low-relief bed waves (LRBW) have been studied in a laboratory flume by Bennett & Bridge (1995b), Livesey (1995) and Livesey *et al.* (1998). LRBW generally have greater heights and lengths than BLS and exist in flows up to where all of bed material is fully mobile. Bennett & Bridge (1995b) concluded that low-relief bed forms were apparently ubiquitous features in channels in which the bed material is composed of sand–gravel mixtures when the bed is not completely mobile. Examples of these bed forms observed in this study are contained in

**Table 1.** Bed forms developed in sand–gravel mixtures.  $\theta$  represents the dimensionless bed shear stress.

Bed form	Height (mm)	Length (mm)	Migration rate (mm sec <sup>-1</sup> )	$\theta$	Texture	References
Particle clusters	$D_{95}$	100–1200	Move by breaking up	0.009	Coarse stoss, fine wake	1
Bedload sheets	4–13	70–1200	1–27	0.04–0.12	Coarse trough, fine stoss coarsens towards crest	2
Low-relief bed waves	8–17	1700–4850	0.3–14	0.04–0.24	Coarse trough, fine stoss coarsens towards crest	3
Dunes	100–100 000	600–100 000	30	0.1–0.3	Fine stoss coarsens towards crest. Coarse trough when sediment transport low	4
Antidunes	10–1000	50–19 000	Direction variable. Rate influenced by steepness	0.2–2.5	Coarest clasts on or near the crest, few on the lee	5
Transverse ribs	1–2 clast diameters	50–1250 (width) 200–2500 (wavelength)	Direction variable	0.2–2.5	Coarse clasts, with fine infill and backfill	6

(1) Dal Cin, 1968; Brayshaw, 1984; Naden & Brayshaw, 1987; Hassan & Reid, 1990; de Jong, 1991; Reid & Hassan, 1992.

(2) Dietrich *et al.*, 1989; Kuhnle & Southard, 1990; Bennett & Bridge, 1995b.

(3) Bennett & Bridge, 1995b; Livesey *et al.*, 1998.

(4) Hubbell *et al.*, 1987; Kuhnle & Southard, 1988; Dinehart, 1989, 1992a,b; Alexander & Fielding, 1997; Carling, 1999.

(5) Kennedy, 1963; Shaw & Kellerhals, 1977; Whittaker & Jaeggi, 1982; Mehrotra, 1983; Yagishita, 1994.

(6) Koster, 1978; McDonald & Day, 1978; Rust & Gostin, 1981; Allen, 1983; Bluck, 1987.

Fig. 6 (below) and more complete explanations will be given below. Formative processes for the bed form populations observed include bed shear stress perturbations, particle interactions between coarse and fine fractions, and bed form amalgamation.

Kleinhans *et al.* (2002) measured bed forms in a laboratory flume and on two rivers with bimodal bed sediment mixtures of sand and gravel. Bed forms that occur when not all of the sizes of the bed material are in motion were the focus of his study. Three bed form types with increasing flow strengths were recognized from flume experiments by Kleinhans *et al.* (2002): flow parallel sand ribbons, barchans and dunes. In sand ribbons, the sand was transported downstream in several flow-parallel strips with non-moving gravel between the strips. The barchans consisted of classic barchanoid shapes separated from each other by barely moving gravel. Kleinhans *et al.* (2002) concluded that for non-uniform sediment, the relevant particle diameters should be derived from the transported sediment rather than the bed sediment. This is important for channels in which the bed material contains a mixture of sand and gravel as the transported sediment may consist of significantly finer diameter particles than the bed material. They also concluded that supply-limited bed forms in the field cannot in general be predicted based on local flow and sediment conditions because of unknown upstream sediment sources.

Carling *et al.* (2000) identified ripples, small and large dunes formed in sand and fine gravel

over a rarely entrained flat gravel lag layer on the River Rhine, Germany. Large dunes were generally found to be three-dimensional barchanoid in shape, while the ripples and small dunes were primarily two-dimensional in planform. A depth limitation rather than a sediment supply limitation was concluded to be the primary control of dune height in this system.

The objectives of this study were to conduct a series of experiments in a laboratory flume with sediment and flow conditions that would produce long and low bed forms that are found in streams with gravel–sand beds such as Goodwin Creek. Laboratory experiments under steady controlled conditions allowed new data to be collected to further elucidate the processes associated with bed forms in conditions of partial transport in streams with gravel–sand beds. Although not an exact match to the data collected on sand–gravel bed forms on Goodwin Creek, the flume-derived data were comparable in terms of bimodal parameters, relative roughness, and shear stress ratios such that the data provides a window to the processes acting in the field.

## EXPERIMENTAL EQUIPMENT AND PROCEDURES

Fourteen mobile bed experiments were conducted in an adjustable slope, recirculating laboratory flume (Fig. 1), with a channel 15.2 m long, 0.356 m wide and 0.457 m deep. Eight of these

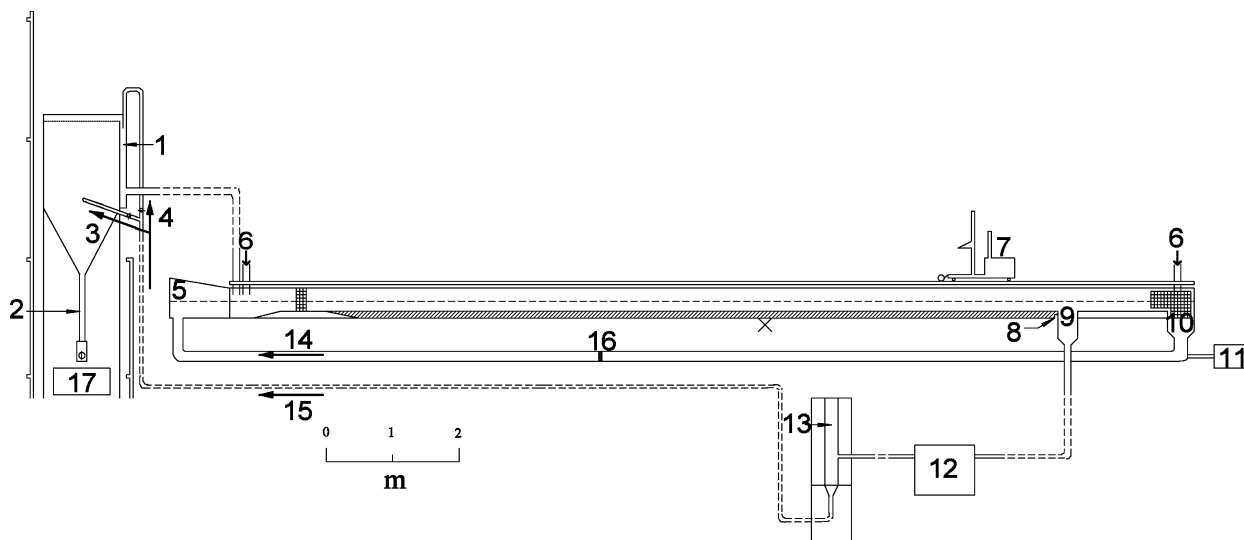


**Fig. 1.** Schematic diagram of the laboratory flume employed. 1, overflow section; 2, accumulation tube; 3, sediment sampling; 4, sediment and water recirculation; 5, headbox; 6, water supply; 7, instrument carriage; 8, sediment retaining wall; 9, sediment trap; 10, tail box; 11, propeller pump; 12, diaphragm pump; 13, surge tank; 14, water recirculation; 15, recirculation of water and sediment; 16, Venturi meter; 17, manometer and standpipes.

experiments employed a water depth of *ca* 0.18 m (series 1), while the remaining six runs used a flow depth of *ca* 0.14 m (series 2). Sediment and water were recirculated separately by a compressed air diaphragm and propeller pump, respectively. The discharge of the propeller pump was determined from a Venturi meter and associated differential pressure transducer. The diaphragm pump was used to recirculate the sediment caught by the 0.356 m wide by 0.356 m long sediment trap. The flow from the diaphragm pump was calibrated and contributed a small fraction of the total flow in the channel.

The sediment bed and water surface elevation (static and dynamic) were measured relative to the flume base using ultrasonic probes mounted on a motorized carriage. Measurements were taken down the centreline of the test section at 8 mm (sediment bed) and 6 mm (water) intervals ( $\pm 1$  mm). The sediment bed and water surfaces were also repeatedly monitored at one point continuously for 5 or 10 min, depending on the bed configuration. For at least one 20 min period in each experiment, two probes were in operation simultaneously at a known distance apart measuring the elevation of the sediment bed. At the end of each experimental run, the morphology of the test section was mapped in detail with an ultrasonic probe.

Samples of the bed load were collected in an accumulation tube after being captured by the sediment trap. The sample was measured volumetrically, and converted to a mass using a previously determined conversion factor. The

samples were then replaced in the flume by an equivalent mass of bulk sediment, and an appropriate volume of water was removed from the main channel to maintain the water depth. Collection periods varied from 60 to 1500 sec depending on the sediment transport rate. At high transport rates more than one sample was obtained. Bed load samples were taken at the end of the experimental run to minimize any negative effects of the potential differences between the grain-size distribution of the sediment sample and the replacement sediment. Samples of suspended sediment were collected in six 20 sec intervals during each experiment using a sampling port from just downstream of the propeller pump. Each water/sediment sample was weighed and replaced. The sediment was separated from the water, dried and weighed.

After the completion of each experimental run, samples and photographs of the sediment surface in the test section were obtained. The sediment bed surface was sampled at various points by employing a clay piston sampler with a diameter of 0.155 m (Kellerhals & Bray, 1971; Parker *et al.*, 1982; Church *et al.*, 1987; Wilcock & Southard, 1989; Diplas & Fripp, 1992; Bennett & Bridge, 1995a). The sampler was pressed firmly onto the surface of the sediment, which adhered to the clay within the sampler. The sediment was separated from the clay by washing the surface of the sample in a 0.18 mm sieve. The samples were dried, sieved at 0.25- $\phi$  intervals and weighed.

Before commencing an experimental run, the bulk sediment mixture (Fig. 2) was completely

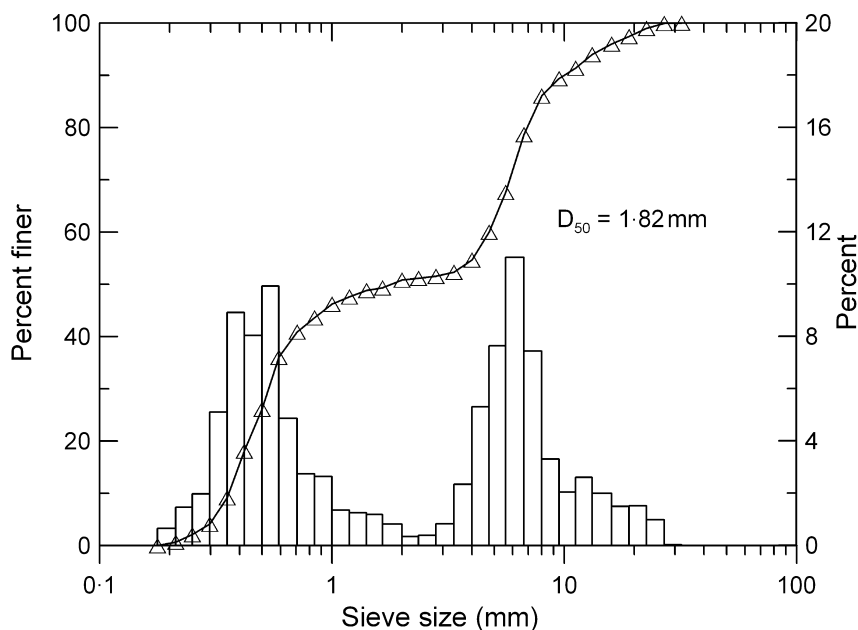


Fig. 2. Bimodal sand-gravel bulk sediment mixture used in the flume experiments.

homogenized and screeded flat, the flume filled with water (22–28 °C), and the flume slope set to 0.007. Uniform, equilibrium flow conditions were established in the flume prior to systematic measurements in the test section, which extended over 2.2 m from 10 m downstream of the headbox to 1.35 m upstream of the sediment trap. The equilibrium stage was identified from successive water and bed surface profiles and observations of bed form geometry stability. Once equilibrium conditions had been achieved (the flume had been running for at least 8 h in all experimental runs), velocity measurements and sediment samples were taken, with concurrent monitoring of bed and water surface elevations. At the end of each experiment, the water was carefully drained from the flume, and the bed surface texture sampled.

### Field site and methods

The field study site was located on the 21.3 km<sup>2</sup> Goodwin Creek Experimental Watershed located in the bluff-line hills of the north-central part of the state of Mississippi, just east of the flood plain of the Mississippi River (Blackmarr, 1995; Alonso & Binger, 2000). The elevation of the watershed ranges from 71 to 128 m above sea level, with a mean channel slope of 0.004. Stream flow is flashy following storm events, and over bank flows are rare because of the large heights of the incised channel banks. The channel at the study site drains 17.9 km<sup>2</sup> of

the watershed and has low base flows except during storm events. Runoff events usually last several hours and occur most commonly during intense convective storms in winter and spring. The channel at the study site is 24 m wide and has a depth of 3.3 m. The bed material has a bimodal size distribution, with a median grain diameter of 8.3 mm and a range of 0.1–60 mm (Kuhnle, 1992) (Fig. 3). The study site has flows several times per year that mobilize the bed material sediment and generate bed forms (Kuhnle *et al.*, 1989).

Bed form data were automatically collected at the study site on Goodwin Creek from a tethered floating platform 4.1 m long and 0.6 m wide. Distances from the platform to the bed were measured at four locations 1.02 m apart in the streamwise direction. An acoustic pulse-echo system was used to record the distance to the bed from the four transducers (numbered S1, S2, S3 and S4 from upstream to downstream) every 23 sec (Kuhnle & Derrow, 1998; Kuhnle, 2000). Distances from a fixed location to the water surface were measured using a sub-aerial acoustic measurement device at intervals of 10 sec. Precipitation, air and water temperature, and flow discharge were collected at station 2 of the Goodwin Creek Experimental Watershed which was located 82 m downstream of the study site. Data from previous studies at this site (Kuhnle & Willis, 1992; Kuhnle, 1992) were used to calculate flow, velocity, boundary shear stress, and grain size of the bed load.

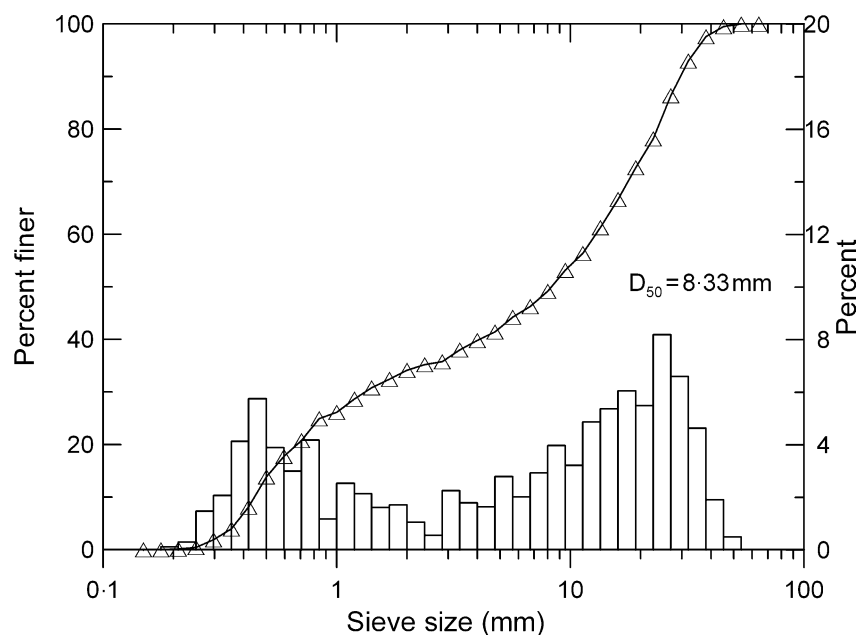


**Fig. 3.** Grain size distribution of the bed material at the Goodwin Creek study site.

The sediment and flow conditions at the field site and laboratory experiments were similar in several ways (Table 2). The bimodal parameters of Wilcock (1993) and Sambrook Smith *et al.* (1997) of the bed material sediments for the laboratory experiments and the field site are both close in value and above the critical values of 1.7 (Wilcock, 1993) and 1.5–2.0 (Sambrook Smith *et al.*, 1997). This indicates that the finer grain sizes in the bed material of the flume and Goodwin site begin moving at measurably smaller values of flow strength than the coarser sizes (Kuhnle, 1993; Wilcock, 1993). The ratios of the flow depth to the median bed material grain size are also similar between the Goodwin site and the flume experiments. Ratios of bed shear stress to the critical shear stress for initiation of motion of the median size of the bed material sediments are also seen (Table 2) to be in a similar range for field and laboratory sites. These comparisons indicate that the sediments in the experiments and at the field site would have been entrained in a similar manner and the resulting bed forms should be similar between the two systems.

## DATA ANALYSIS – LABORATORY EXPERIMENTS

The mean flow depth in the test section  $d$  was determined by subtracting the mean values of the filtered ultrasonic records of bed and water surface elevation at a point. The mean velocity  $U$  was calculated from the flow discharge divided by the cross-sectional flow area. Water surface slope  $S$  was obtained by subtracting the dynamic water surface elevations from the static heights and applying a least-squares linear regression. This procedure was repeated several times for each experiment and an average value calculated. The slope was used to determine the spatially averaged boundary shear stress  $\tau_0$ , from

$$\tau_0 = \rho g R S, \quad (1)$$

where  $\rho$  is fluid density,  $g$  is the acceleration of gravity, and  $R$  is the hydraulic radius (=flow area divided by wetted perimeter).

The height and period of bed forms with discernible relief (more than 2 mm high, and a period >5 sec) were determined for the laboratory data. First the ultrasonic records of bed elevation at a point over time were filtered to remove spikes. Then a moving average of 15 was superimposed before measurements of bed form height and period were taken ( $\pm 0.25$  mm,  $\pm 0.5$  sec). Typically 200 bed forms were used to calculate height and period of the bed forms for each experimental run. Bed form migration rate was determined by correlating bed forms (*ca* 20 for each experimental run) across two simultaneous bed height records, which were taken a known distance apart. This separation distance was divided by the average temporal difference between the two records for the time for the passage of two corresponding bed form parts (i.e. crest to crest). Length of the bed forms was calculated by multiplying the migration rate by the period.

Bed load transport rates were obtained from the average of volumetric and weight measurements taken over known time periods. Moments were calculated for the grain-size distributions of the bed load and surface sediment samples. The suspended sediment transport rate was determined by multiplying the sediment concentration (sediment weight divided by the combined water and sediment weight) by the weight of water being discharged per second, divided by the flume width.

The areal clay-piston surface sediment samples were converted to volumetric values following the procedures from Kellerhals & Bray (1971) with a conversion factor (–0.16), determined from the work of Diplas & Fripp (1992).

## DATA ANALYSIS – FIELD SITE

Boundary shear stress was calculated using Eq. 1 on Goodwin Creek with water surface elevation

**Table 2.** Flow and sediment comparisons between field and laboratory sites.

Study site	$B_w$ – bimodal parameter (Wilcock, 1993)	$B_s$ – bimodal parameter (Sambrook Smith <i>et al.</i> , 1997)	Flow depth to median bed material grain-size ratio ( $d/D_{50}$ )	Shear stress ratio ( $\tau_0/\tau_c$ )
Goodwin Creek	2.7	3.6	70–146	2–6
Laboratory Flume	2.3	4.0	77, 99	2–5

data from four USGS-type bubble gauges connected to pressure transducers over a 91.4 m reach directly upstream from the measurement platform. The water surface data allowed flow depths and slopes to be calculated for the 91.4 m reach on Goodwin Creek.

The bed elevation data collected on Goodwin Creek were analysed for bed forms following Willis (1968). The bed elevation with time records were analysed in pairs for the four adjacent sensors to determine the characteristics of the bed forms. Care was taken to only analyse portions of the bed elevation records where the characteristics of the bed forms did not change significantly over the time considered.

Cross-correlations for the bed elevation records were calculated for lags from zero to one half of the total length of the record. The speed of the bed forms ( $U_d$ ) was determined by:

$$U_d = \frac{l}{t_1}, \quad (2)$$

where  $l$  is the distance between the probes,  $t_1$  is the time that is required for the average dune to move between the two probes. The period of the bed forms ( $\lambda_t$ ) was calculated by the relation:

$$\lambda_t = 2(\Delta x + t_1), \quad (3)$$

where  $\Delta x$  is the negative lag time when the cross-correlation coefficient is minimized (Willis,

1968). The spacing of the bed forms ( $\lambda_x$ ) was then determined as:

$$\lambda_x = \lambda_t U_d. \quad (4)$$

The period, spacing and height (difference between adjacent trough and crest) of bed forms are known to vary significantly even for steady uniform flows (Middleton & Southard, 1984). To accurately determine the characteristics of bed forms, several need to be measured with the same flow conditions. It has been recommended that the record should be 10 times as long as the average period of the bed forms (Willis, 1968). In Goodwin Creek, flows with sufficient magnitude to transport bed material are seldom steady. The data from Goodwin Creek were analysed in sections over which the bed forms showed minimal changes. Twenty-five intervals from 12 runoff events were analysed for this study.

## RESULTS – LABORATORY EXPERIMENTS

Fourteen experiments were completed using two flow depths, with bed shear stresses ranging from 2 to 5 times the critical shear stress and with Froude numbers ranging from 0.3 to 0.8 (Table 3). The range of conditions used was the widest practical with the constraints of the flume for subcritical flows.

**Table 3.** Mean equilibrium hydraulic conditions for laboratory experiments.

Run	$d$ (m)	$U$ (m sec <sup>-1</sup> )	$Q$ (m <sup>3</sup> sec <sup>-1</sup> )	$S$ ( $\times 10^{-3}$ )	$Fr$	$\tau_0$ (Pa)	$Re^*$	Dominant bed form
Series 1								
A	0.172	0.42	0.026	1.87	0.33	1.60	73	FPS
B	0.172	0.52	0.032	1.96	0.40	1.68	75	RLBF
C	0.181	0.59	0.038	2.20	0.44	1.94	80	BLS
D	0.173	0.63	0.039	2.27	0.49	1.95	80	BLS
E	0.176	0.72	0.045	2.65	0.55	2.30	87	BLS
F	0.178	0.74	0.047	3.09	0.56	2.70	94	LRBW
G	0.176	0.78	0.049	3.51	0.60	3.05	100	LRBW
H	0.177	0.83	0.052	4.33	0.63	3.77	112	LRBW
Series 2								
I	0.138	0.51	0.025	2.32	0.44	1.77	77	RLBF
J	0.141	0.58	0.029	2.51	0.49	1.94	80	BLS
K	0.150	0.58	0.031	2.88	0.48	2.30	87	BLS
L	0.142	0.67	0.034	3.59	0.57	2.78	96	LRBW
M	0.139	0.81	0.040	4.89	0.69	3.74	111	LRBW
N	0.141	0.94	0.047	6.08	0.80	4.69	125	LRBW

$d$  is mean flow depth (series 1  $\pm$  2%, series 2  $\pm$  3%);  $U$  is the depth averaged velocity;  $Q$  is mean flow discharge ( $\pm$  3%);  $S$  is water surface slope (series 1  $\pm$  12%, series 2  $\pm$  10%);  $Fr$  is the Froude number,  $\tau_0$  is the bed shear stress obtained from the depth–slope product,  $Re^*$  is the particle Reynolds number =  $[(\tau_0/\rho)^{1/2}D_{50}]/\nu$ , where  $\rho$  and  $\nu$  are the density and kinematic viscosity of water, respectively, and dominant bed forms are FPS (flow parallel strips), RLBF (ripple-like bed forms), BLS (bed load sheets), LRBW (low-relief bed wave) (see text for explanation of bed form types).

### Bed form morphology and dynamics

Cluster analysis was used to determine groupings within the bed form data. Cluster analysis is a multivariate technique which identifies groupings within data sets when the number of groups and group membership are not known. It is an unbiased numerical technique used to classify objects based on multiple parameters. However, there is no underlying theoretical model assumed when using this technique. To classify the observed bed forms into discrete populations, *k*-mean values and hierarchical cluster analysis (aggradational) were performed for each experimental run using the SPSS software package (Anderberg, 1973; Hartigan, 1975; Everitt, 1993; SPSS, 1998). Bed form height and period were directly measured using the ultrasonic probe and were found to be the best variables to separate the bed forms. The procedure first required the logarithm of the bed form height and period to be taken, and these values were then scaled between 0 and 1 to ensure the variables were weighted equally. Hierarchical clustering joins together the closest groups, as determined from the squared Euclidean distance. Once in a cluster a data point cannot be removed from that grouping

*k*-Mean values analysis was repeated for different numbers of cluster centres to support the results from the hierarchical method. The hierarchical method was used on a subset of the data (40 bed forms each time). The cluster analysis

technique identified three distinct bed form populations based on bed form height and period measurements (Fig. 4). The data in Fig. 4 illustrate how the three groups have very little overlap and the relative separation between the groups. Similarity between the groups was represented by the squared Euclidean distance and is illustrated in Fig. 5 for run M. For standardized data the distance coefficients are a measure of the similarity of the objects and groups and are directly related to correlations (Davis, 1973). The three groupings of bed forms identified replace one another as the dominant form as flow strength increases (Fig. 6). Due to inherent variability, bed form populations rather than individuals are discussed here.

At low flow discharges, the sand fraction tended to accumulate in flow parallel strips, migrating across the coarser, immobile particles (e.g. run A: Iseya & Ikeda, 1987; Ferguson *et al.*, 1989; Tsujimoto & Kitamura, 1996; Kleinhans *et al.*, 2002). The stationary ultrasonic probe did not detect the flow parallel strips due to the transitions in roughness occurring in the lateral rather than the longitudinal direction.

As the discharge was increased, the sandy strip regions (up to 3) tended to widen, coalesce into one strip near the centre of the channel, and deform into asymmetrical transverse features. These bed forms were relatively small in height (3–5 mm), length (30–802 mm), and period (16–46 sec), with a relatively high migration rate (4–34 mm sec<sup>-1</sup>).

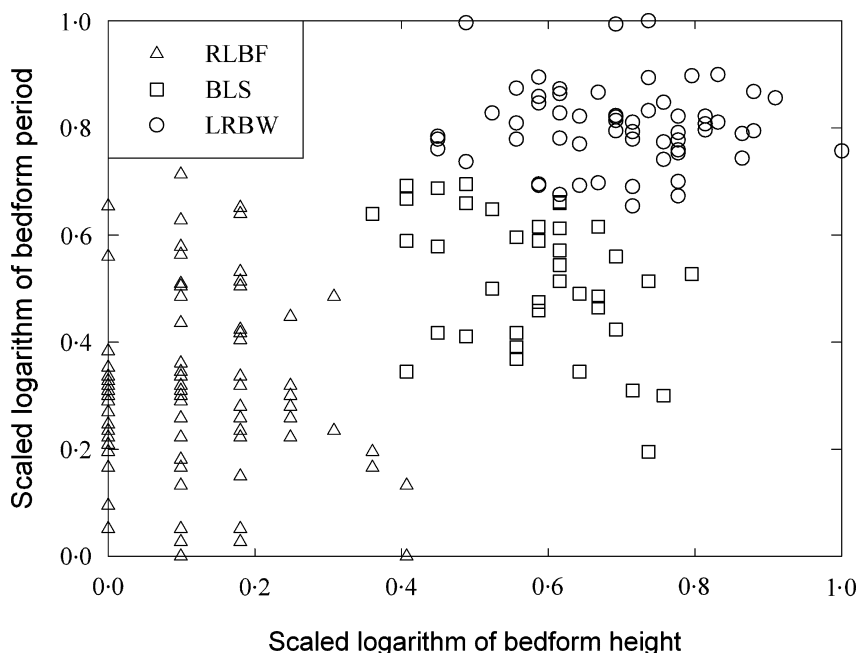


**Fig. 4.** Example plot of bed form period against height for run M illustrating cluster membership. The logarithm of bed form period and height is taken and scaled from 0 to 1. RLBF, BLS and LRBW represent ripple-like bed forms, bed load sheets and low-relief bed waves respectively.

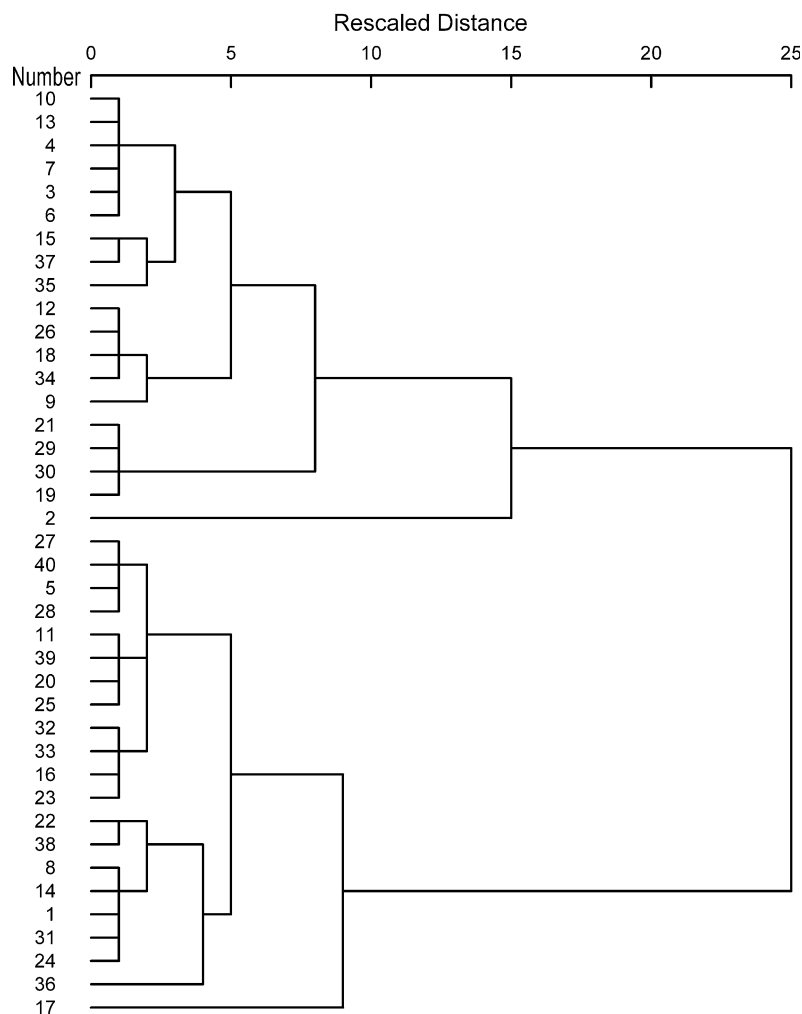


**Fig. 5.** Dendrogram for run M using distance coefficients as a measure of similarity. The lower the value of the distance coefficient, the greater the degree of similarity of the groups.

Their height and period showed no dependence with flow depth. They were characterized by a steep lee side, less steep stoss slope, and a rounded crest, and were observed in every experiment except run A. These features, which were predominantly composed of sand (bed load  $D_{50} = 0.5$  mm), appeared similar to ripples (e.g. Yalin, 1992; Baas, 1999), but were formed by fully rough turbulent flow (Table 3). Due to their similarity to ripple bed forms they will be called ripple-like bed forms (RLBF). Representative profiles of bed forms are illustrated in Fig. 6.

The second bed form population identified by cluster analysis were present at higher bed shear stresses (Fig. 6). These bed features had heights of 7–12 mm, lengths of 71–1061 mm, periods of 30–69 sec, and migration rates of 8–27 mm sec<sup>-1</sup>. These features showed no height or length difference with flow depth. Between the individual forms generally a gravel lag is present. These bed forms share many similarities with previous observations of BLS (Table 4) and were less

regularly spaced and taller than RLBF, which were sometimes superimposed on the stoss side of these forms. BLS were present in all experiments except runs A, B and I.

At the highest flow discharges employed, the largest bed forms (LRBW) developed, the height and migration rate of which were dependent on flow depth (Fig. 6). For flow depths of 180 mm, these bed forms had heights of 13–15 mm and migration rates of 9–14 mm sec<sup>-1</sup>. At depths of 140 mm, heights were 8–10 mm and migration rates were 11–25 mm sec<sup>-1</sup>. Lengths (2.3–4.8 m) and periods (116–256 sec) were not affected by the change in the depth of flow. These bed forms (here termed LRBW) were differentiated from BLS by their greater length, crestal platform and gentle stoss side, on which both BLS and ripples were superimposed. The troughs of the LRBW generally were flat and dominated by a gravel armour, which was mobile at the highest bed shear stresses. LRBW were observed in experimental runs F, G, H, L, M and N.

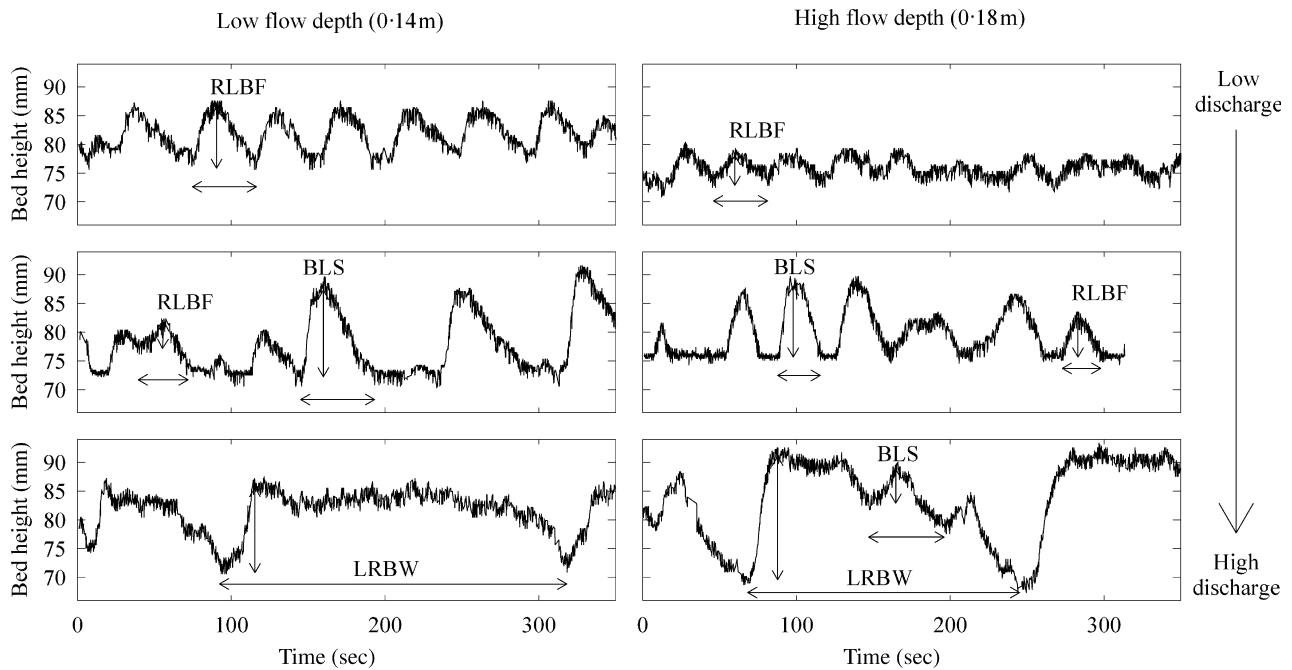


**Fig. 6.** Example bed records over a range of flow depths and discharges. Flow is from right to left. RLBF, BLS and LRBW represent ripple-like bed form, bed load sheet and low-relief bed wave respectively. The height and period of each bed form type is highlighted.

**Table 4.** Morphological and dynamic characteristics of ripple-like bed forms (RLBF), bed load sheets (BLS) and low-relief bed waves (LRBW).

Source	Bed form	$H$ (mm)	$L$ (m)	$p$ (s)	$L/H$ (mean)	$L/d$	$L/p$ (mm sec <sup>-1</sup> )	$D_{50(\text{mm})}$ bed material
Present study	RLBF	3–5	0.03–0.80	16–46	104	2–3	4–34	1.82
	BLS	7–12	0.07–1.06	30–69	60	3–4	8–27	1.82
	LRBW (1)	13–15	2.68–3.89	119–237	234	18–24	9–14	1.82
	LRBW (2)	8–10	2.30–4.85	116–256	397	20–26	11–25	1.82
Goodwin Creek	BLS	65–263	2.73–28.45	378–3178	66	4–24	4–9	8.33
Bennett & Bridge (1995b)	BLS	4–13	0.60–1.20	572–1008	56–338	4–12	1–1.5	2.0
	LR bars	10–17	1.70–2.40	2800–6770	131–200	17–24	0.3–0.9	2.0
Kuhnle (1986)	BLS	2–4	0.5–3	–	583	24–49	5–10	3.03
	Dunes	10	0.6	–	60	9	30	3.03
Whiting <i>et al.</i> (1988)	BLS (Duck Creek)	10–20	0.5–2	–	83	3.6	2–4	4.6
	BLS (Muddy Creek)	2–4	0.2–0.6	–	133	1.3	–	0.9
Dietrich <i>et al.</i> , 1989	BLS	1–2 $D$	–	–	–	–	–	3.7
Wilcock, 1992	BLS ( $MC_{50}$ )	1–2 $D$	1000–2000	–	–	–	–	2.55
	2D dunes ( $MC_{50}$ )	–	800–1200	–	–	–	–	2.55
Livesey (1995)	BLS	1–17	0.01–0.47	43–60	2–60	2.2	2–3	1.07
	LR bed forms	5–25	0.4–1.7	342–1040	70	9.5	0.5–1	1.07

$H$ ,  $L$ ,  $p$  and  $d$  represent bed form height, bed form length, bed form period, and flow depth, respectively.

### Bed form texture and bed load transport

Due to their low relief, bed forms in the flume channel were most noticeable from their charac-

teristic concentrations of fine and coarse bed material. As discharge increased, the mean grain size of the bed load and crestal surface tended to become coarser, whilst the standard deviation

and skewness decreased (Table 5). At the lowest transport rates, the finer and coarser fractions were under-represented in the bed load when compared with their occurrence in the bulk sediment mix. The finer sizes may be under-represented in the bed load due to suspension and hiding effects (Kuhnle, 1993; Wilcock & McArdeell, 1993), whereas coarser particles typically require a greater shear stress for entrainment. As shear stresses were increased, difference in mobility of the size fractions would be expected to be reduced and the size distribution of the bed load and bulk mix should become very similar. This was indeed the case for experiments M and N (Table 5). Experiments C/D and F/G

experienced similar total water discharge, and the grain-size distributions of the bed load are comparable (Table 5) indicating the reproducibility of the results.

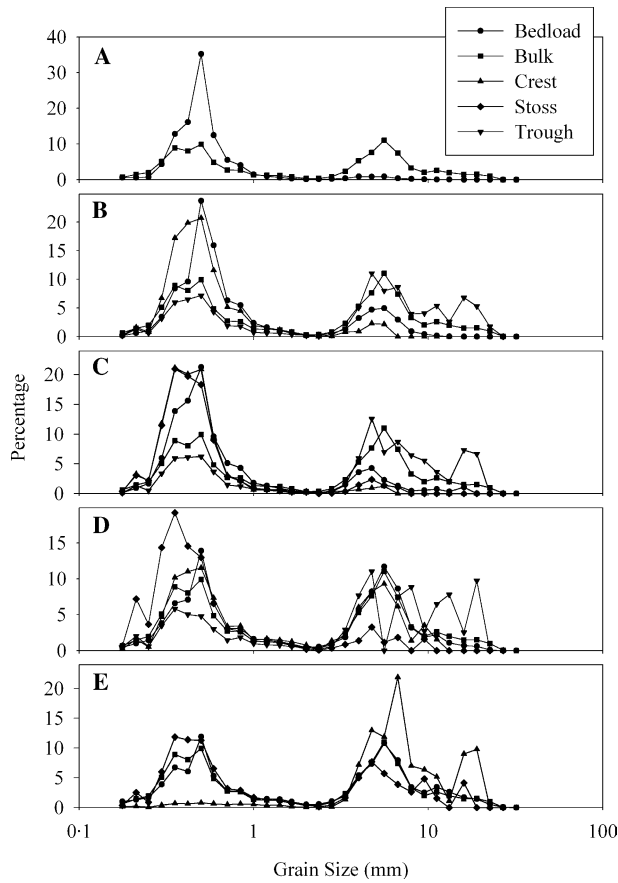
The mean, standard deviation, and skewness of the grain-size distributions for the trough and stoss regions are fairly stable for the ranges of discharges investigated in this study (Table 5). Divergent values may result from the presence of superimposed bed forms on the stoss, and coarse, immobile particles protruding through the thin bed form.

Figure 7 shows representative grain-size distribution curves for the bed load and bulk sediment mixture for several representative experiments.

**Table 5.** Textural characteristics of bed load and bed forms.

	Sample	Percentile (mm)						Mean (mm)	SD (mm)	Skew
		5	16	50	84	90	95			
A	Bulk	0.31	0.41	1.82	7.62	10.07	14.55	1.85	0.25	1.05
	Bed load	0.35	0.41	0.55	0.80	0.91	1.11	0.58	0.65	4.12
B	Bed load	0.36	0.43	0.57	0.83	0.95	1.24	0.62	0.63	4.83
C	Bed load	0.32	0.39	0.55	3.40	4.94	6.42	0.79	0.37	2.88
	Trough	0.35	0.48	5.41	13.29	17.58	19.87	3.40	0.24	0.68
	Crest	0.28	0.35	0.46	0.64	0.74	1.19	0.50	0.58	6.21
	Stoss	0.28	0.35	0.47	0.69	0.98	4.66	0.55	0.49	4.90
	D	Bed load	0.32	0.39	0.57	5.02	6.02	7.07	0.92	0.34
E	Bed load	0.31	0.39	0.72	6.16	6.97	8.14	1.29	0.29	1.33
	Crest	0.30	0.36	0.50	1.25	6.25	10.56	0.72	0.35	3.45
	Stoss	0.32	0.41	4.77	11.61	13.90	15.96	2.41	0.23	0.87
F	Bed load	0.33	0.44	0.73	6.08	6.87	7.94	1.32	0.30	1.37
G	Bed load	0.32	0.41	0.84	6.21	6.97	7.96	1.40	0.29	1.24
	Trough	0.33	0.45	4.81	11.14	13.77	15.60	2.60	0.24	0.82
	Crest	0.37	0.50	4.08	7.15	8.14	9.46	2.17	0.30	0.81
	Stoss	0.30	0.36	0.50	5.55	9.21	14.00	0.85	0.29	2.58
H	Bed load	0.30	0.39	0.88	6.38	7.39	8.97	1.37	0.28	1.30
	Trough	0.34	0.53	5.52	17.68	23.43	25.11	4.16	0.23	0.67
	Crest	0.49	1.15	5.90	11.18	12.65	14.17	4.50	0.35	0.43
	Stoss	0.27	0.35	0.52	1.24	4.00	5.21	0.66	0.42	2.81
I	Bed load	0.34	0.40	0.54	0.73	0.91	1.51	0.59	0.57	6.59
J	Bed load	0.34	0.42	0.57	1.13	4.15	5.65	0.75	0.45	3.34
K	Bed load	0.35	0.44	0.62	4.31	5.50	6.61	0.90	0.38	2.34
	Trough	0.35	0.48	5.32	13.67	17.66	20.35	3.19	0.24	0.75
	Crest	0.32	0.38	0.52	0.85	1.18	4.28	0.60	0.52	4.34
L	Bed load	0.31	0.41	0.78	6.30	7.15	8.46	1.36	0.29	1.33
	Trough	0.34	0.52	5.84	17.67	19.76	21.14	4.00	0.24	0.64
	Stoss	0.25	0.33	0.44	0.71	1.25	5.33	5.33	0.45	4.89
M	Bed load	0.33	0.45	1.95	7.04	8.11	10.73	1.79	0.28	1.05
	Trough	0.33	0.48	5.25	14.60	18.72	20.71	3.56	0.24	0.67
	Crest	0.33	0.41	0.82	6.29	7.24	9.55	1.42	0.29	1.22
	Stoss	0.23	0.31	0.45	0.94	3.39	5.47	0.58	0.41	3.58
N	Bed load	0.31	0.44	2.78	8.20	10.82	14.37	2.03	0.26	0.99
	Crest	1.12	4.83	7.30	16.89	18.95	20.71	7.21	0.45	0.31
	Stoss	0.31	0.39	0.69	7.04	9.68	12.06	1.38	0.26	1.38

SD and skew are standard deviation and skewness of grain-size distribution.



**Fig. 7.** Representative grain-size distributions for an RLBF (A, run I), bed load sheet (B and C, runs K and C) and low-relief bed wave (D and E, runs M and N) bed configurations. Note the difference percentage scales used.

Figure 7A shows grain-size distributions for an experiment (run L) in which the predominant bed form was RLBF. The sediment in motion was predominantly sand, with sizes greater than 16 mm completely immobile. The trough region between the starved bed forms consisted of a static armour layer. The presence of the static armour inhibits erosion in the trough region, limiting bed form height (Richards & Clifford, 1991; Carling *et al.*, 1993; Roden, 1998).

In the experiments when BLS were present (Fig. 7B,C), the sand size fractions were still over-represented in the bed load, although to a lesser extent compared with rippled beds. No sediment larger than 16 mm was found in the bed load indicating that the coarse trough regions were composed of a static armour. The texture of the crest and stoss followed a similar trend to that of the bed load (Fig. 7B,C, Table 5) but with a smaller gravel component.

In the case of LRBW, the grain-size distributions of the crest, bed load, and bulk mixture were

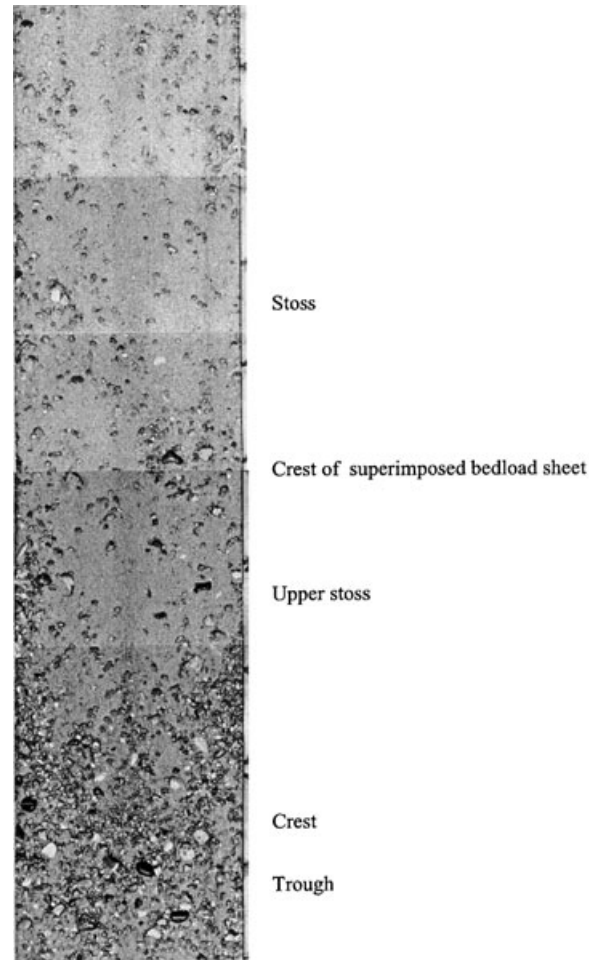


**Fig. 8.** Low-relief bed wave, run M. Flow is from top to bottom. Flume width is 0.356 m.

comparable (Fig. 7D,E). In experiment runs M and N (Fig. 7D,E), the transition from partial transport to full transport of all sizes in the bulk mix is illustrated. The size distribution of the crest exhibited a concentration of coarse grains, while the sediment on the stoss was largely composed of sand (Table 5, Fig. 8). The data shown in Fig. 7 confirm that as the flow strength increased, the bed load and crestal regions of the bed forms coarsened, and the bed forms increased in height.

The surface along the stoss was shown to coarsen for LRBW as the crest was approached (Fig. 9, Table 6). However, the stoss remained significantly finer than the trough and crest regions. As the mean grain size increased, the skewness and standard deviation of the distribution were reduced along the stoss. It was not possible to investigate the textural variations within stoss regions of individual RLBF and BLS in this study due to their short length.

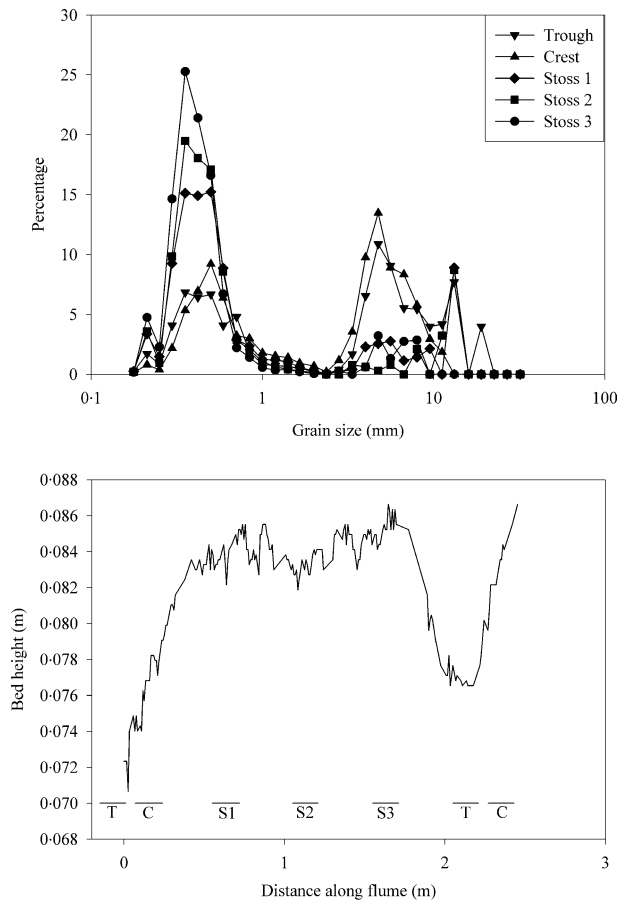


Fig. 9. Textural variations over a low-relief bed wave, run G, series 1.

### Suspended sediment

The sediment that passed over the sediment trap in the flume was defined as being in suspension. At a discharge of  $0.025 \text{ m}^3 \text{ sec}^{-1}$  the level of suspended sediment was minimal at both flow depths. However, for the experiments with higher flow discharges the transport of suspended sediment was observed to increase exponentially (Fig. 10), contributing up to 8% (more typically 1–3%) of the total sediment transport. The exponential increase was greatest under the experiments with the 0.14 m flow depths. The standard deviation of the suspended sediment sample concentrations also increased with increasing discharge.

## RESULTS – FIELD SITE

From June, 1997 to March, 1999, bed elevation and flow data were collected and analyzed from 25 events on Goodwin Creek. Flow depths ranged from 0.39 to 1.21 m, bed shear stresses ranged

from 2 to 6 times the critical shear stress, and Froude numbers ranged from 0.16 to 0.24 (Table 7). An example bed height record collected on Goodwin Creek is shown in Fig. 11.

The bed forms identified from echo sounding records on Goodwin Creek had lengths from 3 to 28 m, periods from 400 to 3000 sec, and heights from 0.06 to 0.25 m (Kuhnle & Derrow, 1998; Kuhnle, 2000). Bed forms were long and low with length-to-height ratios of 30 to 135 (mean = 66.1). Bed form period and spacing showed no relation with boundary shear stress, while bed form height did show evidence for a relation with shear stress (Figs 12 and 13). The bed forms on Goodwin Creek did not separate into logical groups based on height, length, or period. A more workable grouping was made between bed forms that formed below or above the shear stress (30 Pa, Fig. 14) which indicated all sizes of the bed material were fully mobilized. Bed forms at shear stresses below 30 Pa, would consist of BLS and LRBW, with a BLS occurring at shear stresses <20 Pa and LRBW occurring at shear stresses from 20–30 Pa. RLBF were too small in height to be resolved on Goodwin Creek.

Textural data on the sizes of sediment that composed the bed forms in Goodwin Creek were not available due to the near impossibility of collecting samples of the bed forms during a runoff event. However, bed load transport data collected at the site (Kuhnle & Willis, 1992; Kuhnle, 1992) indicate that the change in the size distribution with increasing flow strength (Fig. 14) is similar to that observed in the experiments conducted in the laboratory flume and the associated bed forms in field and flume were also probably similar.

## DISCUSSION

### Bed form length and time scales

In the present experiments the width/depth ratios were 2 and 2.5 for series 1 and 2, respectively. To evaluate the effect of width/depth ratios on the flow, the secondary circulation in the laboratory flume when empty of sediment (to remove the effect of a changing boundary) was determined using an acoustic Doppler velocimeter with a 2-dimensional side-looking probe. Flow measurements were collected for one half of the channel width at a lateral and vertical spacing of *ca* 1 cm (Horton, 2001). With a flow depth of 0.18 m and depth averaged velocity of  $0.29 \text{ m sec}^{-1}$ , the lateral velocity did not exceed 5.2% of the downstream

**Table 6.** Textural variations over a low-relief bed wave.

Sample	Percentile						Mean	SD	Skew
	5	16	50	84	90	95			
Run G, series 1									
Trough	0.33	0.45	4.81	11.14	13.77	15.60	2.60	0.24	0.82
Crest	0.37	0.50	4.08	7.15	8.14	9.46	2.17	0.30	0.81
Stoss1	0.29	0.36	0.53	5.74	10.29	14.36	0.92	0.28	2.35
Stoss2	0.23	0.36	0.49	1.27	11.28	13.77	0.78	0.29	3.16
Stoss3	0.25	0.33	0.43	0.59	0.67	0.94	0.55	0.40	4.68
Run M, series 2									
Trough	0.33	0.48	5.25	14.60	18.72	20.71	3.56	0.24	0.67
Crest	0.33	0.41	0.82	6.29	7.24	9.55	1.42	0.29	1.22
Stoss1	0.27	0.35	0.52	1.49	4.53	5.81	0.69	0.40	2.71
Stoss2	0.24	0.32	0.46	1.57	5.09	7.77	0.66	0.36	3.00
Stoss3	0.22	0.27	0.39	0.58	0.71	1.42	0.44	0.53	2.77

SD and skew represent standard deviation and skewness of the grain-size distribution.

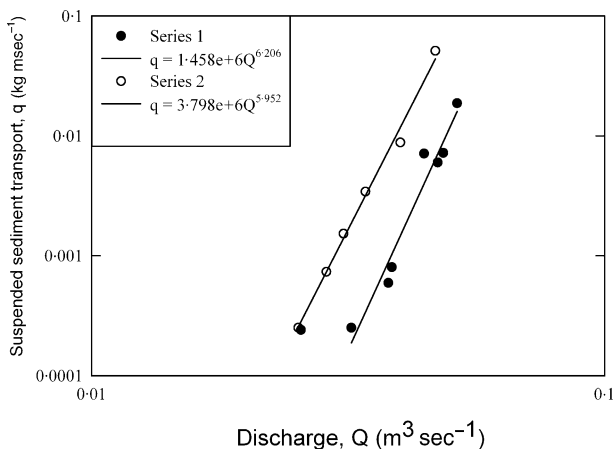


**Fig. 10.** Suspended sediment transport in the flume experiments.

value. For a flow depth of 0.15 m and a depth averaged velocity of 0.18 m sec<sup>-1</sup> the equivalent figure was 5.7%. However the cross-stream velocity was typically a much smaller percentage of the downstream velocity component, although the depth averaged velocities generated in the experimental runs were considerably larger.

Figure 15 highlights the fact that both the length and period of RLBF and BLS are similar. These two features are morphologically distinguished by their height, which is greater for the BLS. LRBW are longer than the other two bed form populations identified. Their height is directly related to the flow depth as seen by the changes from series 1 to 2 data (Table 4), and under the present flow conditions is either similar or greater than that of the BLS.

Ripple-like bed forms exhibit the greatest migration rate, followed by BLS and then LRBW,

implying that an increase in height corresponds with a fall in bed form celerity. However, viewing all the points as a whole on Fig. 15C, there is no obvious relationship between bed form height and celerity. Higher migration velocities tend to be associated with smaller BLS. Furthermore, the velocity of the LRBW is greater when shallower flow prevails and their height is reduced. The maximum migration rate of the LRBW under the highest flow depth investigated is approximately half that of the BLS. The experiments of Bennett & Bridge (1995b) confirm this, although the actual magnitude of the migration rates differ. This result is in agreement with the observation of superimposed BLS traversing the stoss of the slow-moving LRBW.

### Effect of flow on bed form geometry and texture

With increasing discharge, the length and migration rate of RLBF and BLS tends to increase slightly (Fig. 16). LRBW also travel at a greater velocity with increasing discharge, but their period diminishes (Bennett & Bridge, 1995b). The rate of increase in bed form celerity is greater when the flow is shallower (series 2). There is no obvious trend in bed form height with rising discharge, with the exception of BLS which diminish in height under the shallower flow conditions (series 2).

As discharge increases the mean grain size of the bed load and crestal region increases (Fig. 17). This effect is enhanced under shallower flow conditions (series 2), where bed shear stresses are greater for a given discharge (Table 3). Rapid

**Table 7.** Summary of bed form data collected on Goodwin Creek.

Data number	$d$ (m)	$U$ (m sec <sup>-1</sup> )	$Q$ (m <sup>3</sup> sec <sup>-1</sup> )	$Fr$	$\tau_0$ (Pa)	$Re^*$	$F$
063097	1.03	0.69	16.59	0.22	23.48	1272	0.38
082097	0.81	0.54	10.01	0.19	18.06	1115	0.47
011598	0.77	0.51	7.94	0.19	16.50	1066	0.48
021098a	0.58	0.39	2.76	0.16	12.11	913	0.61
021098b	0.71	0.47	6.17	0.18	15.12	1021	0.52
021098c	0.64	0.43	4.30	0.17	13.56	967	0.56
021698a	0.66	0.43	4.40	0.17	13.66	970	0.56
021698b	0.67	0.45	5.14	0.17	14.29	992	0.55
030598a	0.58	0.39	2.48	0.16	11.84	903	0.61
030598b	0.65	0.43	4.12	0.17	13.41	961	0.56
030598c	0.83	0.56	10.06	0.19	18.11	1117	0.45
030598d	0.77	0.51	8.22	0.19	16.71	1073	0.48
030798a	0.75	0.50	8.02	0.18	16.56	1068	0.51
030798b	1.19	0.80	23.48	0.23	32.41	1494	0.39
030798c	0.88	0.59	12.44	0.20	19.94	1172	0.45
031798a	0.64	0.43	3.96	0.17	13.26	956	0.56
031798b	0.76	0.51	7.62	0.19	16.24	1058	0.48
042798a	0.65	0.43	9.55	0.17	17.72	1105	0.73
042798b	1.11	0.74	23.25	0.22	32.00	1485	0.45
030299	0.63	0.42	3.60	0.17	12.94	944	0.56
030699	0.68	0.45	4.84	0.18	14.03	983	0.52
031399a	1.05	0.70	20.76	0.22	28.04	1390	0.44
031399b	1.21	0.81	24.81	0.24	35.65	1567	0.42
031399b2	1.21	0.81	24.57	0.23	34.98	1552	0.41
031399c	0.75	0.49	7.47	0.18	16.14	1054	0.51

Symbols are the same as for Table 3.

coarsening of the crest is linked to the development of LRBW, which first occur at a lower discharge under the shallower flow conditions. The texture of the trough seems to remain fairly similar under a wide range of conditions, whereas the stoss region exhibits no obvious trend.

### Relation of bed form geometry to bed load and suspended load

At all discharges, regions of distinct roughness transitions were apparent (see also Ikeda & Iseya, 1988). These roughness transitions are thought to result in alterations of the turbulent flow structure

(Robert *et al.*, 1992; Livesey, 1995), which may in turn affect sediment transport at the local scale (Best, 1996). This is illustrated by BLS and LRBW, which are discernible by variations in transport rate along their length (Kuhnle, 1986; Iseya & Ikeda, 1987; Kuhnle & Southard, 1988; Whiting *et al.*, 1988). Observations from video footage taken during the experiments indicate that once entrained from the trough/stoss boundary, the coarser particles tend to travel farther and faster compared with the sand fractions, and are deposited or decelerated just downstream of the crest. Kuhnle & Southard (1988) found that the peak in the transport rate of the coarse fractions

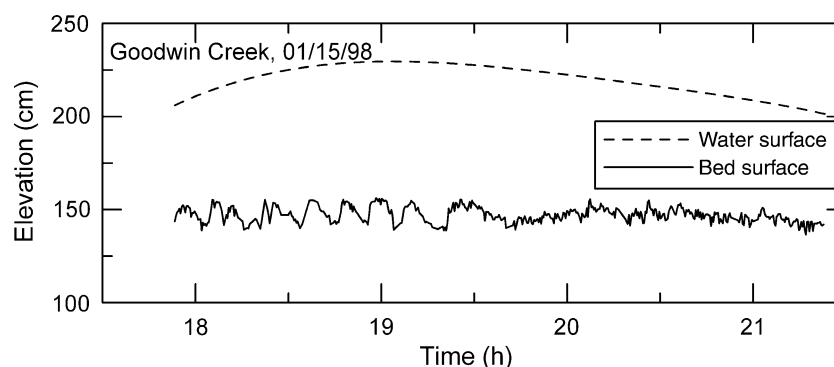


**Fig. 11.** Example bed surface elevation data collected on Goodwin Creek for runoff event of 15 January 1998.

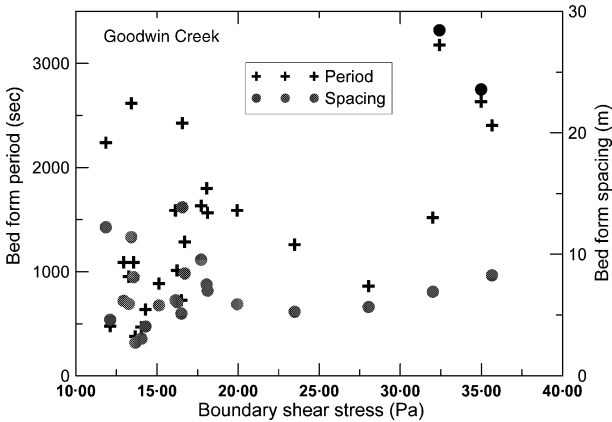


Fig. 12. Bed form period and spacing versus boundary shear stress for Goodwin Creek.

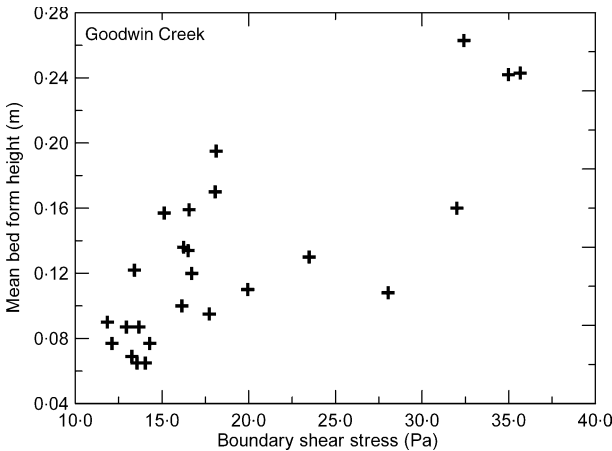


Fig. 13. Bed form height versus boundary shear stress, Goodwin Creek.

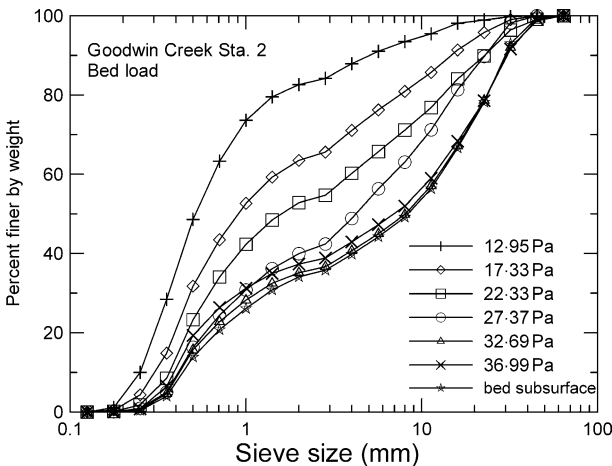


Fig. 14. Changes in size distribution of bed load for increasing shear stress, Goodwin Creek, station 2 (Blackmarr, 1995).

occurred shortly before the maximum transport rate for the total bed load and the sand component. The bed load transport peaks were also related to the passage of the crest by Kuhnle & Southard (1988), which has a similar composition to the bed load. Maximum transport rates for the finer sand fractions are associated with the movement of the fine grained stoss. The sand transport peak may be delayed due to these size fractions infilling the voids in the coarse trough (Iseya & Ikeda, 1987). Furthermore, the fine sediment buried beneath the coarser clasts can only be exposed to the flow once the larger grains have been entrained (Kuhnle & Southard, 1988). The stoss side of the LRBW were observed to fine in the upstream direction in the present experiments (Table 6, Fig. 9), which may explain why Kuhnle & Southard (1988) measured the maximum transport rate being further delayed for decreasing sand size fractions. In the case of BLS and LRBW, Bennett & Bridge (1995b) found that the approach of the bed form crest also caused the water surface to dip. Consequently, Whiting *et al.* (1988) determined that BLS and LRBW migration cause periodic variations in bed shear stress and bed load transport rate of up to an order of magnitude. Several studies have shown that where BLS are superimposed on LRBW, secondary fluctuations in bed load flux can be observed (Gomez *et al.*, 1989; Bennett & Bridge, 1995b; Livesey *et al.*, 1998).

In the case of BLS and LRBW, the crest and bed load exhibited a similar grain-size distribution, indicating that all sediment sizes were transported within a migrating bed form. Grain size samples from the surface of RLBF could not be collected due to their small size relative to the area sampled using the clay piston technique. However, visual observations and the grain-size distribution of the bed load indicate that ripples were composed mainly of sand. The average bed load sediment transport rate,  $q_{bf}$ , for the highest order bed form observed in each experimental run was calculated (Simons *et al.*, 1965; Crickmore, 1970; van Rijn, 1993) using the following equation:

$$q_{bf} = \beta(1 - \rho_s)\rho ch, \tag{5}$$

where  $\beta$  is the shape factor (i.e. the fraction of a rectangle, equivalent in height and length to the bed form, which is occupied by the bed form),  $\rho_s$  is the porosity factor (0.4 for poorly sorted coarse sand; van Rijn, 1993),  $\rho$  is the sediment density ( $2650 \text{ kg m}^{-3}$ ),  $c$  is the average bed form migration rate and  $h$  is mean bed form height. In order to calculate a value for the shape factor, 20 examples

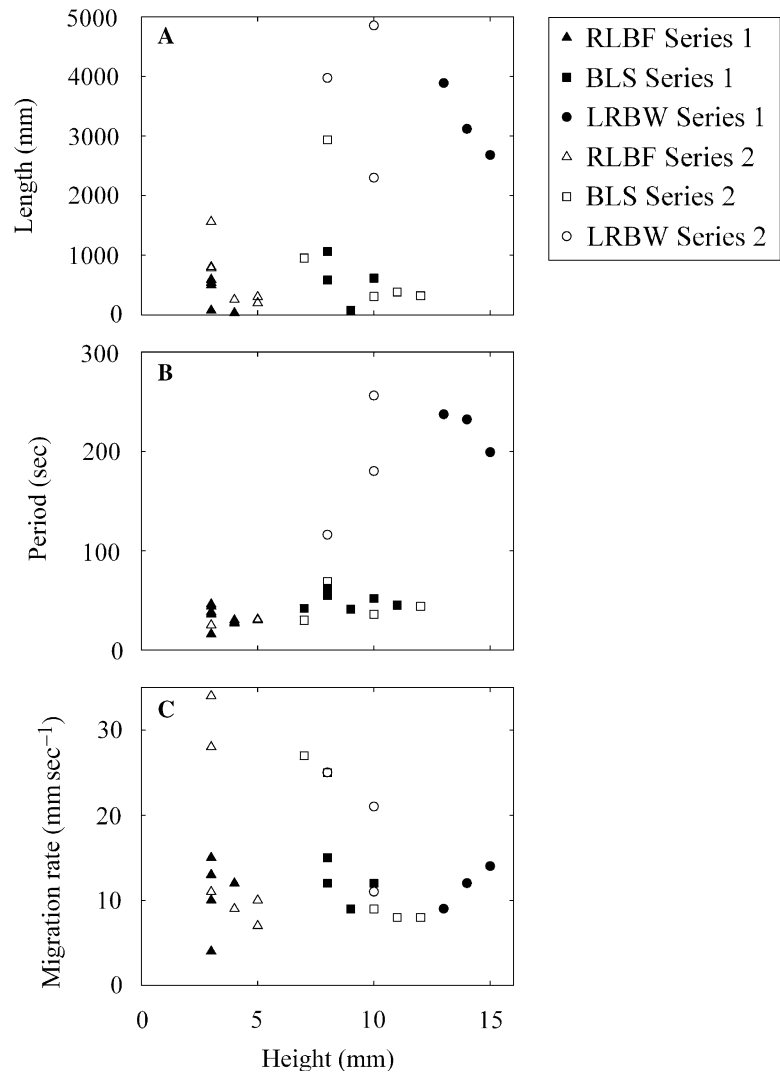


**Fig. 15.** Bed form height versus bed form length, period, and migration rate.

of each bed form type were traced and superimposed. An average value for the shape factor was calculated from the largest and smallest resulting features. The shape factor was found to vary between 0.41 and 0.80, with average values of 0.51, 0.50, 0.61 and 0.70 for ripples, BLS, LRBW in series 1 and LRBW in series 2, respectively.

Estimates of bed load transport rates from Eq. 5 are compared with measured values for total sediment transport rates in Fig. 18. At discharges below  $ca\ 0.045\ m^3\ sec^{-1}$  (bed load transport rate of  $0.1\ kg\ ms^{-1}$ ) total sediment transport is accommodated by the migration of ripples and BLS. At higher discharges LRBW develop, and bed form migration no longer completely accounts for total sediment transport. Additional contributions to total sediment transport may include grains moving independently of the bed forms, even longer low-relief bed forms not recognized here and sediment in suspension.

### Conceptual framework for sediment transport in bimodal mixtures

The preceding results, and synthesis with the literature, can be used to propose a conceptual framework for the evolution of bed forms in bimodal mixtures. In bimodal mixtures, the relatively fine grain sizes are entrained first, forming isolated longitudinal stripes of finer material (Iseya & Ikeda, 1987; Ferguson *et al.*, 1989; Parker, 1991; Robert *et al.*, 1992; Nezu & Nakagawa, 1993; Tsujimoto & Kitamura, 1996; Tsujimoto, 1999; Kleinhans *et al.*, 2002). As these sandy patches grow in volume, coalesce, and migrate over a static armour consisting of the coarse size fractions, they eventually develop into RLBF. With further increases in mean bed shear stress, larger clasts are entrained and incorporated into the RLBF, especially at the upstream limit of the stoss side. Isolated gravel clasts were

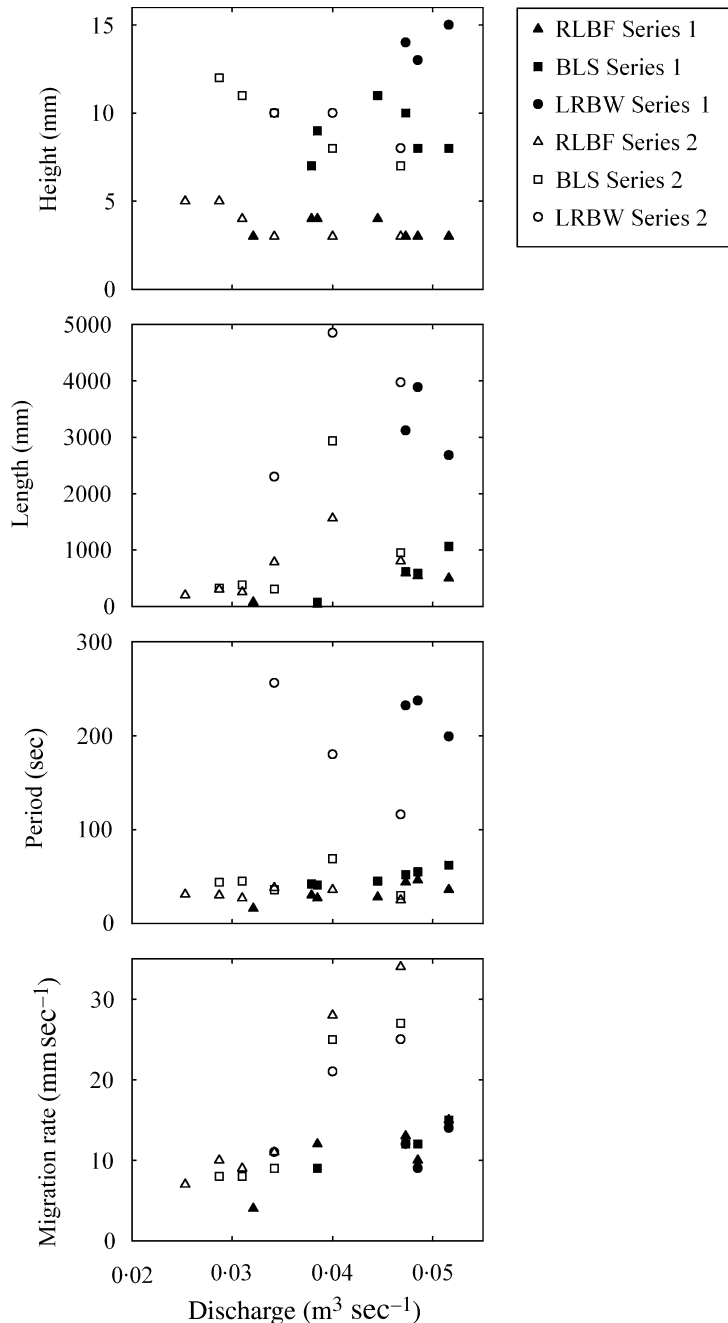


**Fig. 16.** Variations in bed form height, length, period, and migration rate with discharge.

observed to be entrained at distinct roughness transitions (e.g. the boundary of the fine grained stoss and the coarse armour layer) and proceed quickly along the sandy stoss of the bed forms, this being promoted by a low friction angle and high relative protrusion.

With increasing flow strength, RLBF develop into BLS as the bed load incorporates more clasts of larger size, although a static armour remains in the bed form trough. The increased mean size of sediment in transport may be responsible for changing the grain roughness within the bed

form, altering the flow structure, and making more sediment available to the bed forms, thus increasing the height of BLS compared with RLBF. Further increases in the quantity and calibre of mobile sediment are accommodated by the development of LRBW that are associated with a slight increase in bed form height and substantial increase in wavelength (Wilcock & McArdell, 1993; Coleman & Melville, 1994). As coarser particles are increasingly prone to transport as flow strength increases, the armoured trough eventually becomes mobile. LRBW stu-

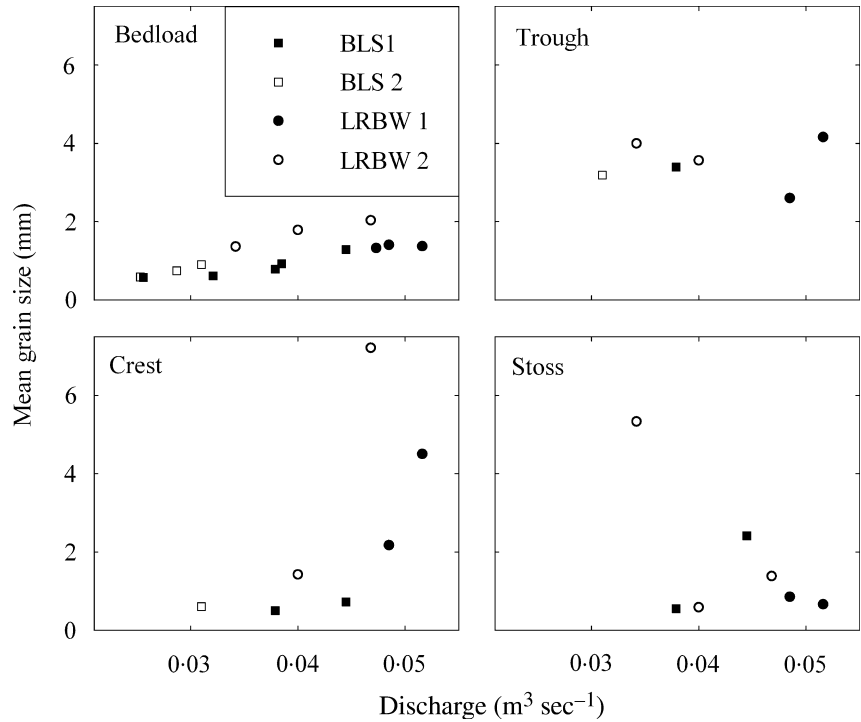


Fig. 17. Variations in mean grain size of bed load and specific bed form areas with discharge.

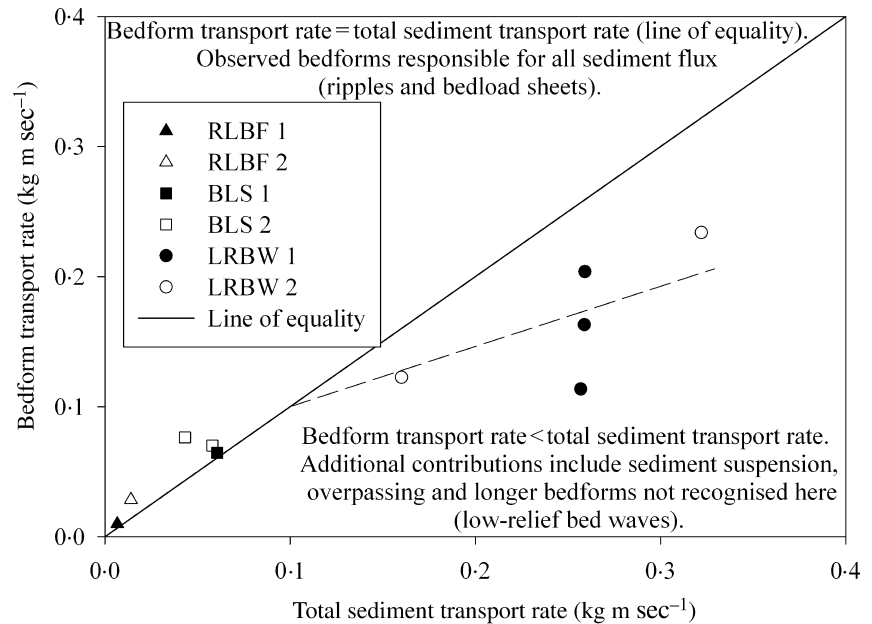


Fig. 18. Comparison of bed load and bed form transport rate.

died in series 2 (shallower flow conditions) and BLS are approximately equivalent in height to the  $D_{90}$  (10.07 mm) of the bulk bimodal sediment mixture, whereas LRBW observed in series 1 are equal in height to the  $D_{95}$  (14.55 mm). The maximum grain size of the bed load was 13.2, 19 and 26.9 mm for RLBF, BLS and LRBW, respectively. On Goodwin Creek the maximum size of the sediment in transport shows only

slight changes with increasing flow strength; however, the fraction of the coarse sizes in transport changed markedly as shown by the median size of the bed load which changed progressively from 0.52 to 8.06 mm as flow strength increased (Fig. 14). Bed form height increased with increasing flow strength in the field as more of the larger sizes of the bed material were entrained. When coarser clasts are transpor-

ted, they experience greater exposure to the flow, increase bed roughness and change the turbulent flow structure. As flow strength increases, the additional volume of sediment entrained and transported is also accommodated by increases in bed form length. However, it appears that the wavelength is not regulated by any large-scale flow structures such as flow separation and suggests grain roughness effects may still be critical. The growth of bed forms occurs by bed form amalgamation as a result of the greater proportion of the bed material that is available for transport as the larger grain sizes are entrained.

The majority of the clasts transported over a BLS or LRBW were deposited in the trough region, becoming buried by the advancing bed form and subsequently re-exposed and entrained following the passage of the bed form (i.e. a dune-like grain path, Wilcock & McArdell, 1993). However, as shear stress increased and BLS and LRBW developed, the finest fractions were transported in suspension, whilst the coarsest grains were carried as bed load over several bed forms. Sediment suspension and gravel over-passing thus make it difficult to define the area of the bed contributing to bed load transport (e.g. a bed form unit), as sediment in transport over a specific bed form is not necessarily entrained from that feature, especially in the case of LRBW (Wilcock & McArdell, 1993). Furthermore, the occurrence of different sediment transport mechanisms also leads to variability in bed form wavelength.

### The link with dunes

Bed load sheets are thought to be genetically related to two-dimensional dunes which develop in well-sorted, coarse sand (Costello & Southard, 1980; Wilcock & Southard, 1989; Raudkivi & Witte, 1990; Ditchfield & Best, 1992; Best, 1996). The flow and sediment conditions from the laboratory and field studies were plotted on velocity-size diagrams for given ranges of flow depth (Southard & Boguchwal, 1990). It is not clear which grain size should be considered as representative for bed forms that occur on beds composed of a wide mixture of sizes that have the potential for partial transport. The data employed by Southard & Boguchwal (1990) were from narrow size distributions with all sizes in transport. The data in this study were plotted in two ways, using the median size in transport and the median size of the bed material as references. The

data from the flume experiments, with the exception of 1 point, all plotted in the dune stability region (Fig. 19A). The data from Goodwin Creek plotted in or near the dune stability region when the grain size in transport was used. Every value from Goodwin Creek plotted in the lower plane region when the median size of the bed material was used as the representative grain size (Fig. 19A,B). Using the grain size of the bed load to represent the bed forms, as advocated by Kleinhans *et al.* (2002), seems to indicate that all bed forms encountered in this study are dunes; however, characteristics related above such as bed form height not being dependent on flow depth or shear stress and only partial entrainment of the bed material would argue against the smaller bed forms (RLBF, BLS) being classified as dunes.

The heights of both the LRBW from the laboratory channel and the bed forms from Goodwin Creek showed evidence for being positively related with flow depth. The large fraction of the bed that was immobile at lower flows in the flume channel restricted the ability of the bed forms to change in height with flow strength. Dunes have been observed to develop from BLS (Kuhnle & Southard, 1988; Whiting *et al.*, 1988; Wilcock, 1992), and exhibit a similar length to flow depth ratio (*ca* 5). Large macroturbulent flow structures associated with dune bed forms are absent or not effective for two-dimensional dunes and the bed forms observed here. This is manifested by the long length/height ratios of the bed forms (especially BLS and LRBW) which indicates that if there is flow separation and a trapped eddy at the bed form crest, it is not sufficiently strong to locally entrain sediment that will initiate the next bed form. It is our belief (also see Bennett & Bridge, 1995b) that the bed forms that formed at the higher flow strengths when all of the sizes of the bed in the field and flume channels were fully mobile were dunes. The ones that occurred at the lower flows were sediment starved and probably should not be classified as dunes. These bed forms (RLBF, BLS, some LRBW) may reasonably be labelled as a precursor to dunes that occur in channels with bed materials composed of bimodal mixtures of sand and gravel when not all of the sizes of the bed material are in motion.

### CONCLUSIONS

With increasing bed shear stress the following bed form populations were observed in labora-

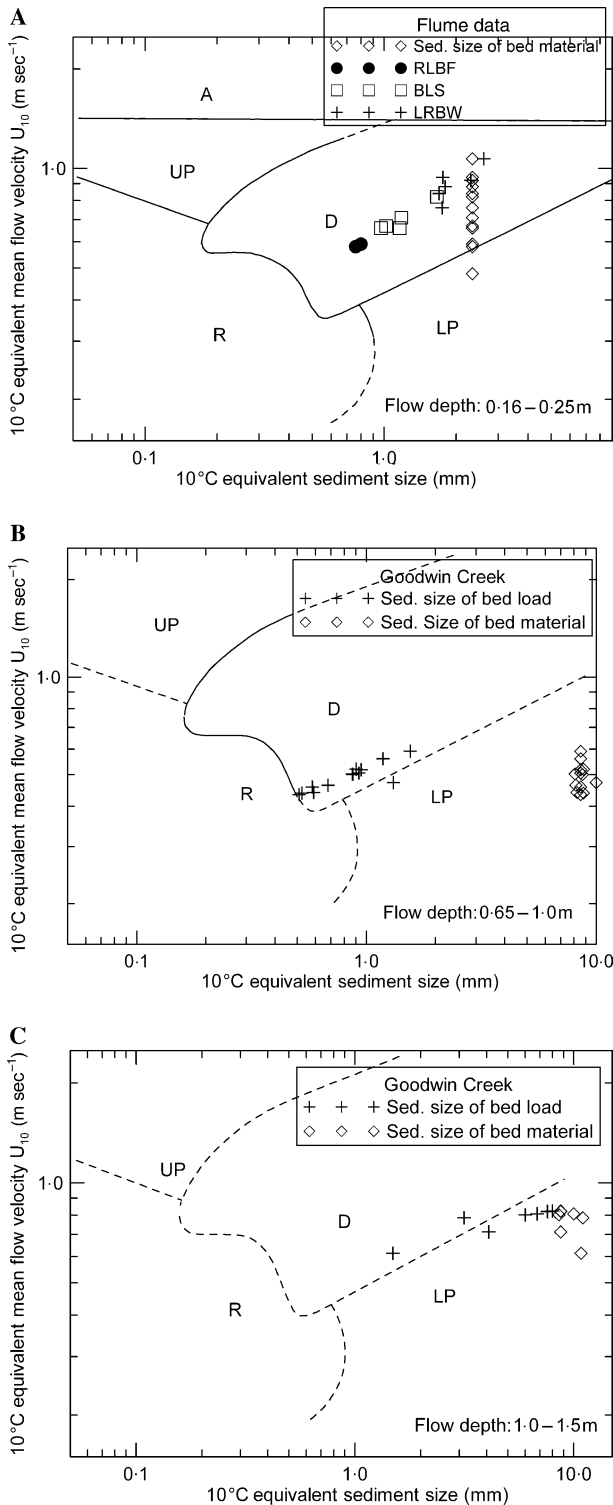


**Fig. 19.** Data from this study plotted in bed form stability diagrams from Southard & Boguchwal (1990). Stability fields: A, antidunes; UP, upper plane bed; D, dunes; LP, lower plane bed; R, ripples. (A) Data from flume experiments with bed form types plotted separately with reference grain size as the bed load  $D_{50}$ . (B, C) Data from Goodwin Creek for flow depths 0.65–1.0 and 1.0–1.5 m respectively.

tory experiments: RLBF (up to 5 mm high and 802 mm long), BLS (up to 12 mm high and 1061 mm long) and LRBW (up to 10–15 mm high, dependent on flow depth, and 4849 mm long). The latter two bed form types have received little detailed attention in the literature, due to their relatively recent recognition. The bed forms were identified from their morphological dimensions (i.e. height and period) using the multivariate technique of cluster analysis. The RLBF were not observed in the field because their size was too small to be measured by available techniques. Bed forms corresponding to BLS and LRBW (mean length = 8.48 m, range = 2.73–28.4 m; mean height = 0.130 m, range = 0.065–0.263 m) were observed on Goodwin Creek.

The extensive laboratory data set presented here enables variations in bed form morphology and texture to be documented over a wide range of discharges, from near incipient motion to just below critical flow conditions. With increasing shear stress the similar grain-size distributions of the crest and bed load both coarsen, and the dynamics of the armour layer change. The morphology of the bed forms remained relatively stable over the range of discharges investigated here. However, the height of the LRBW was dependent on flow depth. The data collected on bed forms from Goodwin Creek also maintained a stable morphology over the range of measured flow conditions. Fractional bed load transport data collected from an earlier study on Goodwin Creek indicate that the bed forms probably change in texture in a similar manner to that observed in the laboratory.

Fluctuations in both total and fractional bed load transport in the laboratory are related to bed form migration. This is supported by the similar nature of the bed load and bed form crest grain-size distributions, and the correspondence of bed load and bed form transport rates (both fractional and total). RLBF have periods up to 46 sec and migrate at up to 34 mm sec<sup>-1</sup>. The period of BLS extends to 69 sec, and their maximum velocity is 27 mm sec<sup>-1</sup>. LRBW are characterized by a period of up to 256 sec and a maximum celerity of 25 mm sec<sup>-1</sup>. The variations in migration rate allow superimposition of features and bed form amalgamation. The bed forms on Goodwin Creek, when scaled by the ratio of mean flow depths between laboratory and field (5:1) were similar in dimensions to those from the flume and it was concluded that changes in size and rate of bed load are controlled by bed form migration. Bed

form periods on Goodwin Creek ranged from 378 to 3178 sec, celerities ranged from 3.4 to 9.7 mm sec<sup>-1</sup>.

A conceptual model of sediment transport in a bimodal mixture is presented. Sediment within the bed forms moves through cycles of entrainment, transport, deposition, burial, and entrainment. Exceptions to this are the finer particles that are transported in suspension and the coarsest particles that, once entrained, can rapidly traverse several bed forms before being deposited. With increases in bed shear stress, these alternative transport mechanisms become more predominant. The bed forms that form before all sizes of the bed are fully mobile are controlled by the amount of sediment available for transport. When all sizes of the bed are fully mobile, dune bed forms result.

## ACKNOWLEDGEMENTS

The research of this study was supported in part by Natural Environment Research Council Research studentship grant no. GT04/97/131/FS to Joanne Horton. John Cox provided valuable assistance in setting up and maintaining the equipment necessary to run the experiments.

## REFERENCES

- Alexander, J. and Fielding, C. (1997) Gravel antidunes in the tropical Burdekin River, Queensland, Australia. *Sedimentology*, **44**, 327–337.
- Allen, J.R.L. (1983) A simplified cascade model for transverse stone-ribs in gravelly streams. *Proc. Roy. Soc. London*, **A385**, 253–266.
- Alonso, C.V. and Binger, R.L. (2000) Goodwin creek experiment watershed: a unique field laboratory. *J. Hyd. Eng.*, **126**, 174–177 (Forum Article).
- Anderberg, M.R. (1973) *Cluster Analysis for Applications*. Academic Press, London, 359 pp.
- Baas, J.H. (1999) An empirical model for the development and equilibrium morphology of current ripples in fine sand. *Sedimentology*, **46**, 123–138.
- Bennett, S.J. and Bridge, J.S. (1995a) An experimental study of flow, bedload transport and bed topography under conditions of erosion and deposition and comparison with theoretical models. *Sedimentology*, **42**, 117–146.
- Bennett, S.J. and Bridge, J.S. (1995b) The geometry and dynamics of low-relief bed forms in heterogeneous sediment in a laboratory channel, and their relationship to water flow and sediment transport. *J. Sed. Res.*, **A65**, 29–39.
- Best, J.L. (1996) The fluid dynamics of small-scale alluvial bedforms. In: *Advances in Fluvial Dynamics and Stratigraphy* (Eds P.A. Carling and M.R. Dawson), pp. 67–125. John Wiley and Sons Ltd, Chichester.
- Blackmarr, W.A. (Ed.) (1995) *Documentation of Hydrologic, Geomorphic, and Sediment Transport Measurements on the Goodwin Creek Experimental Watershed, Northern Mississippi, for the Period 1982–1993*. Research Report No. 3. USDA-ARS, National Sedimentation Laboratory, Oxford, MS.
- Bluck, B.J. (1987) Bed forms and clast size changes in gravel-bed rivers. In: *River Channels: Environment and Process* (Ed. K. Richards), pp. 159–178. Blackwell, Oxford.
- Brayshaw, A.C. (1984) Characteristics and origin of cluster bedforms in coarse-grained alluvial channels. In: *Sedimentology of Gravels and Conglomerates*, Vol. 10 (Eds E.H. Koster and R.J. Steel), pp. 77–85. Canadian Society of Petroleum Geologists Memoir, Calgary, AB.
- Bridge, J.S. and Bennett, S.J. (1992) A model for the entrainment and transport of sediment grains of mixed sizes, shapes, and densities. *Water Resour. Res.*, **28**, 337–363.
- Carling, P.A. (1999) Subaqueous gravel dunes. *J. Sed. Res.*, **69**, 534–545.
- Carling, P.A., William, J.J., Glaister, M.G. and Orr, H.G., (1993) *Particle Dynamics and Gravel-Bed Adjustments*. Final technical report #DA JA45-90-C-0006. European Research Office of the Army, London, UK. p. 46.
- Carling, P.A., Golz, E., Orr, A.G. and Radecki-Pawlik, A. (2000) The morphodynamics of fluvial sand dunes in the River Rhine, near Mianz, Germany. I. Sedimentology and morphology. *Sedimentology*, **47**, 227–252.
- Church, M.A., McLean, D.G. and Wolcott, J.F. (1987) River bed gravels: sampling and analysis. In: *Sediment Transport in Gravel-Bed Rivers* (Eds C.R. Thorne, J.C. Bathurst and R.D. Hey), pp. 43–87. John Wiley and Sons Ltd, Chichester.
- Coleman, S.E. and Melville, B.W. (1994) Bed-form development. *J. Hydraul. Eng.*, **120**, 544–560.
- Costello, W.R. and Southard, J.B. (1980) Flume experiments on lower-flow-regime bed forms in coarse sand. *J. Sed. Petrol.*, **51**, 849–864.
- Crickmore, M.J. (1970) Effect of flume width on bed-form characteristics. *J. Hydraul. Eng.*, **96**, 473–496.
- Dal Cin, R. (1968) “Pebble clusters”: their origin and utilization in the study of palaeocurrents. *Sed. Geol.*, **2**, 233–241.
- Davis, J.C. (1973) *Statistics and Data Analysis in Geology*. John Wiley and Sons, Inc., New York, 550 pp.
- Dietrich, W.E., Kirchner, J.W., Ikeda, H. and Iseya, F. (1989) Sediment supply and the development of the coarse surface layer in gravel-bedded rivers. *Nature*, **340**, 215–217.
- Dinehart, R.L. (1989) Dune migration in a steep, coarse-bedded stream. *Water Resour. Res.*, **25**, 911–923.
- Dinehart, R.L. (1992a) Evolution of coarse gravel bed forms: field measurements at flood stage. *Water Resour. Res.*, **28**, 2667–2689.
- Dinehart, R.L., (1992b) Gravel-bed deposition and erosion by bed form migration observed ultrasonically during storm flow, North Fork Toutle River, Washington. *J. Hydrol.*, **136**, 51–71.
- Dinehart, R.L. (1999) Correlative velocity fluctuations over a great river bed. *Water Resources Research*, **35**, 569–582.
- Diplas, P. and Fripp, J.B. (1992) Properties of various sediment sampling procedures. *J. Hydraul. Eng.*, **118**, 955–970.
- Ditchfield, R. and Best, J.L. (1992) Discussion: Development of bed features. *J. Hydraul. Eng.*, **118**, 647–655.
- Everitt, B.S. (1993) *Cluster Analysis*. Edward Arnold, London, 170 pp.
- Ferguson, R.I., Prestegard, K.L. and Ashworth, P.J. (1989) Influence of sand on hydraulics and gravel transport in a braided gravel bed river. *Water Resour. Res.*, **25**, 635–643.

- Gomez, B., Naff, R.L. and Hubbell, D.W.** (1989) Temporal variations in bedload transport rates associated with the migration of bedforms. *Earth Surf. Proc. Land.*, **14**, 135–156.
- Hartigan, J.A.** (1975) *Clustering Algorithms*. John Wiley and Sons, London, 351 pp.
- Hassan, M.A. and Reid, I.** (1990) The influence of microform bed roughness elements on flow and sediment transport in gravel bed rivers. *Earth Surface Processes and Landforms*, **15**, 739–750.
- Horton, J.K.** (2001) *Flow and bedform dynamics of a bimodal sand-gravel mixture*. PhD Dissertation, School of Earth Science, University of Leeds, Leeds, UK.
- Hubbell, D.W., Stevens, H.H., Jr, Skineer, J.V. and Beverage, J.P.** (1987) Laboratory data on coarse-sediment transport for bedload-sampler calibrations. *U.S. Geol. Surv. Water Supply Pap.*, **2299**, 31pp.
- Ikeda, H. and Iseya, F.** (1988) *Experimental Study of Heterogeneous Sediment Transport*. Environmental Research Center Papers no. 12, Tsukuba, Japan.
- Iseya, F. and Ikeda, H.** (1987) Pulsations in bedload transport rates induced by a longitudinal sediment sorting: a flume study using sand and gravel mixtures. *Geografiska Annaler*, **69A**, 15–27.
- de Jong, C.** (1991) A reappraisal of the significance of obstacle clasts in cluster bedform dispersal. *Earth Surf. Proc. Land.*, **16**, 737–744.
- Kellerhals, R. and Bray, D.I.** (1971) Sampling procedures for coarse fluvial sediments. *J. Hydraul. Eng.*, **97**, 1165–1180.
- Kennedy, J.F.** (1963) The mechanics of dunes and antidunes in erodible-bed channels. *J. Fluid Mech.*, **16**, 521–544.
- Kleinhans, M.G., Wilbers, A.W.E., De Swaaf, A. and Van den Berg, J.H.** (2002) Sediment supply-limited bedforms in sand-gravel bed rivers. *J. Sed. Res.*, **72**, 629–640.
- Koster, E.H.** (1978) Transverse ribs: their characteristics, origin and paleohydraulic significance. In: *Fluvial Sedimentology*, Vol. Memoir 5, (Ed. A.D. Miall), pp. 161–186. Canadian Society of Petroleum Geologists, Calgary, AB.
- Kuhnle, R.A.** (1986) *Experimental studies of heavy-mineral transportation, segregation, and deposition in gravel-bed streams*. PhD Thesis, Massachusetts Institute of Technology, Cambridge, MA.
- Kuhnle, R.A.** (1992) Fractional transport rates of bedload on Goodwin Creek. In *Dynamics of Gravel Bed Rivers* (Eds P. Billi, R.D. Hey, C.R. Thorne and P. Tacconi), pp. 141–155. J. Wiley and Sons Ltd, Chichester, UK.
- Kuhnle, R.A.** (1993) Incipient motion of sand-gravel sediment mixtures. *J. Hydraul. Eng.*, **119**, 1400–1415.
- Kuhnle, R.A.** (2000) Bed forms in a sand-gravel stream with unsteady flows. In: *ASCE Water Resources Conference Proceedings*, Minneapolis, MN, USA p. 6.
- Kuhnle, R.A. and Derrow, R.W., II** (1998) Automatic measurement of bed height records in a gravel bed stream. In: *Proceedings of the Bouyoucos on Agroacoustics*, Third Symposium, Tishomingo, Mississippi, pp. 23–35.
- Kuhnle, R.A. and Southard, J.B.** (1988) Bed load transport fluctuations in a gravel bed laboratory channel. *Water Resour. Res.*, **24**, 247–260.
- Kuhnle, R.A. and Southard, J.B.** (1990) Flume experiments on the transport of heavy minerals in gravel-bed streams. *J. Sed. Petrol.*, **60**, 687–696.
- Kuhnle, R.A. and Willis, J.C.** (1992) Mean size distribution of bed load on Goodwin Creek. *J. Hydraul. Eng.*, **118**, 1443–1446.
- Kuhnle, R.A., Willis, J.C. and Bowie, A.J.** (1989) Variations in the transport of bed load sediment in a gravel-bed stream, Goodwin Creek, Northern Mississippi, U.S.A. In: *Proceedings of the Fourth International Symposium on River Sedimentation*, Beijing, China, pp. 539–546.
- Livesey, J.** (1995) *Flow structure, bedform development and sediment transport in mixed sand and gravel*. Unpublished PhD Thesis, University of Leeds, Leeds.
- Livesey, J., Bennett, S.J., Ashworth, P.J. and Best, J.L.** (1998) Flow, sediment transport and bedform dynamics in a bimodal sediment mixture. In: *Gravel-Bed Rivers in the Environment* (Eds P.C. Klingeman, R.L. Beschta, P.D. Komar and J.B. Bradley), pp. 149–176. Water Research Publication, Highlands Ranch, CO, USA.
- McDonald, B.C. and Day, T.J.** (1978) An experimental flume study on the formation of transverse ribs. *Geol. Surv. Can. Pap.*, **78-1A**, 441–451.
- Mehrotra, S.C.** (1983) Antidune movement. *J. Hydraul. Div.*, **109**, 302–304.
- Middleton, G.V. and Southard, J.B.** (1984) *Mechanics of Sediment Movement*. S.E.P.M. Short Course no. 3, 2nd edn. S.E.P.M., Tulsa, OK, 401 pp.
- Naden, P.S. and Brayshaw, A.C.** (1987) Small- and medium-scale bedforms in gravel-bed rivers. In: *River channels: Environment and Process*, (Ed. K. Richards), Blackwell, Oxford, UK, p. 249–271.
- Nezu, I. and Nakagawa, H.** (1993) *Turbulence in Open-Channel Flows*. A.A. Balkema, Rotterdam, 281 pp.
- Parker, G.** (1991) Some random notes on grain sorting. In: *International Grain Sorting Seminar*, Vol. Mitteilungen 117 (Eds D. Vischer and M. Jäggi), pp. 1–58. ETH Zurich, Ascena, Switzerland.
- Parker, G., Klingeman, P.C. and McLean, D.G.** (1982) Bedload and size distribution in paved gravel-bed streams. *J. Hydraul. Div.*, **108**, 544–571.
- Raudkivi, A.J. and Witte, H.H.** (1990) Development of bed features. *J. Hydraul. Eng.*, **116**, 1063–1079.
- Reid, I. and Hassan, M.A.** (1992) The influence of microform bed roughness elements on flow and sediment transport in gravel bed rivers: a reply. *Earth Surf. Proc. Land.*, **17**, 535–538.
- Richards, K. and Clifford, N.** (1991) Fluvial geomorphology: structured beds in gravelly rivers. *Prog. Phys. Geogr.*, **15**, 407–422.
- van Rijn, L.C.** (1993) *Principles of Sediment Transport in Rivers, Estuaries and Coastal Seas*. Aqua Publications, Amsterdam.
- Robert, A., Roy, A.G. and De Serres, B.** (1992) Changes in velocity profiles at roughness transitions in coarse grained channels. *Sedimentology*, **39**, 725–735.
- Roden, J.E.** (1998) *The sedimentology and dynamics of mega-dunes, Jamuna River, Bangladesh*. PhD Thesis, University of Leeds, Leeds.
- Rust, B.R. and Gostin, V.A.** (1981) Fossil transverse ribs in Holocene alluvial fan deposits, Depot Creek, South Australia. *J. Sed. Petrol.*, **51**, 441–444.
- Sambrook Smith, G.H., Nicholas, A.P. and Ferguson, R.I.** (1997) Measuring and defining bimodal sediments: problems and implications. *Water Resour. Res.*, **33**, 1179–1185.
- Shaw, J. and Kellerhals, R.** (1977) Paleohydraulic interpretation of antidune bedforms with applications to antidunes in gravel. *J. Sed. Petrol.*, **47**, 257–266.
- Simons, D.B., Richardson, E.V. and Nordin, C.F.** (1965) Bedload equations for ripples and dunes. *U.S. Geol. Surv. Prof. Pap.*, **462-H**, 9 pp.

- Snishchenko, B.F., Muhamedov, A.M. and Mazhidov, T.S.** (1989) Bedload composition effect on dune shape parameters and on flow characteristics. In: *Proceedings of the International Association for Hydraulic Research, 23rd Congress*, Ottawa, Canada, Vol. B, Fluvial Hydraulics, pp. B-105–B-112.
- Southard, J.B. and Boguchwal, L.A.** (1990) Bed configuration in steady unidirectional water flows. Part 2. Synthesis of flume data. *J. Sed. Petrol.*, **60**, 658–679.
- SPSS** (1998) Cluster analysis. In: *SPSS Base 8.0 Applications Guide*. SPSS Inc, Chicago, IL, 372 pp.
- Tsujimoto, T.** (1999) Sediment transport processes and channel incision: mixed size sediment transport, degradation and armouring. In: *Incised River Channels: Processes, Forms, Engineering, and Management* (Eds S.E. Darby and A. Simon), pp. 37–66. John Wiley and Sons, Chichester.
- Tsujimoto, T. and Kitamura, T.** (1996) Interaction between cellular secondary currents and lateral alternate sorting. In: *Coherent Flow Structures in Open Channels* (Eds P.J. Ashworth, S.J. Bennett, J.L. Best and S.J. McLelland), pp. 359–374. John Wiley & Sons Ltd, Chichester.
- Whiting, P.J., Dietrich, W.E., Leopold, L.B., Drake, T.G. and Shreve, R.L.** (1988) Bedload sheets in heterogeneous sediment. *Geology*, **16**, 105–108.
- Whittaker, J.G. and Jaeggi, M.N.R.** (1982) Origin of step-pool systems in mountain streams. *J. Hydraul. Div.*, **108**, 758–773.
- Wilcock, P.R.** (1992) Experimental investigation of the effect of mixture properties on transport dynamics. In: *Dynamics of Gravel-Bed Rivers* (Eds P. Billi, R.D. Hey, C.R. Thorne and P. Tacconi), pp. 109–139. John Wiley and Sons Ltd, Chichester.
- Wilcock, P.R.** (1993) Critical shear stress of natural sediments. *J. Hydraul. Eng.*, **19**, 491–505.
- Wilcock, P.R.** (1997) The components of fractional transport rate. *Water Resour. Res.*, **33**, 247–258.
- Wilcock, P.R. and Kenworthy, S.T.** (2002) A two-fraction model for the transport of sand/gravel mixtures. *Water Resour. Res.*, **38**, 1-21–12-12. #1121.
- Wilcock, P.R. and McArdeell, B.W.** (1993) Surface-based fractional transport rates: mobilization thresholds and partial transport of a sand-gravel sediment. *Water Resour. Res.*, **29**, 1297–1312.
- Wilcock, P.R. and Southard, J.B.** (1989) Bed load transport of mixed size sediment: fractional transport rates, bed forms, and the development of a coarse bed surface layer. *Water Resour. Res.*, **25**, 1629–1641.
- Willis, J.C.** (1968) A lag-deviation method for analyzing channel bed forms. *Water Resour. Res.*, **4**, 1329–1334.
- Yagishita, K.** (1994) Antidunes and traction-carpet deposits in deep-water channel sandstones, Cretaceous, British Columbia, Canada. *J. Sed. Res.*, **A64**, 34–41.
- Yalin, M.S.** (1992) *River Mechanics*. Pergamon Press, Oxford, 219 pp.

*Manuscript received 26 August 2004; revision accepted 29 June 2005*